ZEOLITE CATALYSTS FOR THE CATALYTIC CRACKING OF HIGHER OLEFINS TO BASIC PETROCHEMICALS

BY

AMR ABDALLA IBRAHIM ABDALLA

A Thesis Presented to the

DEANSHIP OF GRADUATE STUDIES

KING FAHD UNIVERSITY OF PETROLEUM & MINERALS

DHAHRAN, SAUDI ARABIA

In Partial Fulfillment of the
Requirements for the Degree of

MASTER OF SCIENCE

In

CHEMICAL ENGINEERING

DECEMBER 2016

KING FAHD UNIVERSITY OF PETROLEUM & MINERALS

DHAHRAN- 31261, SAUDI ARABIA

DEANSHIP OF GRADUATE STUDIES

This thesis, written by **AMR ABDALLA IBRAHIM ABDALLA** under the direction his thesis advisor and approved by his thesis committee, has been presented and accepted by the Dean of Graduate Studies, in partial fulfillment of the requirements for the degree of **MASTER OF SCIENCE IN CHEMICAL ENGINEERING.**

Dr. Sulaiman Al-Khattaf
(Advisor)

Dr. Mohammed Ba-Shammakh
Department Chairman

Dr. Mohammed Ba-Shammakh
(Member)

Dr. Salam A. Zummo
Dean of Graduate Studies

Dr. Mohammad Hossain
(Member)

29/12/16
Date

Dedicated to my parents and my brothers

for their attitude, help and unlimited support throughout my life.

ACKNOWLEDGMENTS

I would like to express my appreciation to King Fahd University of Petroleum & Minerals for granting me the opportunity to pursue my graduate studies at the Chemical Engineering Department. Also, I wish to acknowledge the help provided by my thesis advisor Dr. Sulaiman Al-Khattaf during my research work. I am thankful to my committee members Dr. Mohammed Ba-Shammakh and Dr. Mohammed Mozahar Hossain for their suggestions and advices.

At the end, I would like to express my sincere gratitude to my mother, my father, my brothers and my close friends for their unfailing support and persistent encouragement throughout my entire life.

TABLE OF CONTENTS

LIST OF TABLES

LIST OF FIGURES

LIST OF ABBREVIATIONS AND NOMENCLATURE

AAGR	:	Average Annual Growth Rate
FCC	:	Fluid Catalytic Cracking
LPG	:	Liquefied Petroleum Gas
PDH	:	Propane Dehydrogenation
MTO	:	Methanol to Olefin
MTP	:	Methanol to Propylene
VGO	:	Vacuum Gasoil
P/E	:	propylene over ethylene ratio
PID	:	Proportional –Integral-Derivative
WHSV	:	Weight Hourly Space Velocity
GHSV	:	Gas Hourly Space Velocity
TOS	:	Time On Stream
GC	:	Gas Chromatographic
FID	:	Flame Ionized Detector
CLD	:	Chemical Liquid Deposition
XRD	:	X-ray Diffraction

BET	:	Brunauer-Emmett-Teller
BJH	:	Barrett-Joyner-Halenda
SEM	:	Scanning Electron Microscopy
FTIR	:	Fourier Transform Infrared
TPD	:	Temperature Programmed Desorption
TGA	:	ThermoGravimetric Analyzer
$\mathbf{V_{mic}}$	:	Micropore Volume
$\mathbf{V_{tot}}$	:	Total Volume
$\boldsymbol{k_{i0}}$	:	Pre-exponential factor of the reaction i
$\boldsymbol{E_i}$	:	Activation energy of the reaction i
$\boldsymbol{Y_i}$	:	Mole fraction of lump *i*
T	:	Reaction temperature
$\mathbf{T_o}$	:	Average temperature of the experiments
R	:	Universal gas constant
SS	:	Sum of Squares

ABSTRACT

Full Name : Amr Abdalla Ibrahim Abdalla

Thesis Title : Zeolite Catalysts for The Catalytic Cracking of Higher Olefins to Basic Petrochemicals

Major Field : Chemical Engineering

Date of Degree : December 2016

Higher olefin cracking is investigated to produce propylene as on-purpose propylene technology in order to meet the growing global demand of propylene. Surface modification of ZSM-5 catalyst was carried out by silica deposition using chemical liquid deposition (CLD) method as well as core-shell silicalite composite material by hydrothermal method. The modified ZSM-5 catalyst was characterized using various physiochemical methods such as XRD, TPD, N_2 adsorption-desorption and SEM analysis. Catalytic cracking of 1-butene was carried out using modified ZSM-5 catalysts. The propylene yield was higher for core-shell silicalite composite as compared to silica deposition through CLD method. Silica deposited using CLD method showed propylene-to-ethylene (P/E) ratio of 1.7, whereas core-shell silicalite composite resulted in P/E ratio of 3.0. The higher catalytic activity of core-shell silicalite composite can be attributed to weak acid sites and effective control of external acid sites, which reduces the hydrogen transfer reactions that form alkanes and aromatics. The effective external surface passivation was verified using catalytic cracking of triisopropyl benzene. The core-shell silicalite composite showed excellent stability over 50 hours for the cracking of 1-butene stream. Kinetic modeling was

developed for the ZSM-5 with SiO_2/Al_2O_3 of 1500 based on experiments performed in fixed bed reactor at a temperature range 250-400^{0}C. MATLAB program used power law model to estimate the kinetic parameters.

ملخص الرسالة

الاسم الكامل: عمرو عبدالله إبراهيم عبدالله

عنوان الرسالة: المحفزات الزيوليتية المستخدمة في التكسير الحفزي للأولفينات العليا إلى البتروكيماويات الأساسية

التخصص: هندسة كيميائية

تاريخ الدرجة العلمية: ديسمبر 2016

تتم دراسة تكسير الأوليفنات العليا لإنتاج البروبيلين كتقنية مستهدفة للبروبلين كمنتج أساسي من أجل تلبية الطلب العالمي المتزايد للبروبيلين. في هذه الدراسة، تم تعديل سطح العامل الحفاز ZSM-5 عن طريق ترسيب السيليكا بإستخدام طريقة ترسيب السائل الكيمايائي (CLD) و كذلك تم التعديل بواسطة الهيكلة-الجوهرية لمركب مادة السيليكالايت بإستخدام طريقة حرارية مائية. العوامل الحفازة المعدلة تم توصيفها بإستخدام طرق فيزيوكيميائية مختلفة مثل: حيود الأشعة السينية , الإمتزاز مبرمج درجة الحرارة TPD، إمتصاص و إمتزاز النتروجين و تحليل مجهر المسح الإلكتروني. تم إجراء التكسير الحفزي لعنصر 1-بيوتين بإستخدام عوامل الحفازة (ZSM-5) المعدلة. تم التوصل إلى أن إنتاجية البروبيلين كانت لي للعامل الحفاز المعدل التعديل بواسطة الهيكلة-الجوهرية لمركب مادة السيليكالايت بالمقارنة مع العامل الحفاز المعدل عن طريق ترسيب السيليكا بإستخدام طريقة ترسيب السائل الكيمايائي. أظهر العامل الحفاز المعدل عن طريق ترسيب السيليكا بإستخدام طريقة ترسيب السائل الكيمايائي نسبة بروبيلين إلى إيثيلين تساوي 1.7 بينما كانت تلك النسبة للعامل الحفاز المعدل التعديل بواسطة الهيكلة-الجوهرية لمركب مادة السيليكالايت تساوي 3.0. النشاط الحفزي العالي للعامل الحفاز المعدل التعديل بواسطة الهيكلة-الجوهرية لمركب مادة السيليكالايت يمكن أن يعزى للمواقع الحمضية الضعيفة و السيطرة الفعالة على المواقع الحمضية الخارجية، مما يقلل تفاعلات نقل الهيدروجين التي تؤدي إلي تكوين الألكانات و العطريات. تم التحقق من فعالية السطح الخارجي بإستخدام التكسير الحفزي ل Triisopropylbenzene. و أظهر العامل الحفاز المعدل التعديل بواسطة الهيكلة-الجوهرية لمركب مادة السيليكالايت أستقرار ممتاز على مدى 50 ساعة لتكسيير عنصر 1-بيوتين. تم توضيح النماذج الحركية للعامل الحفاز ZSM-5 بنسبة سليكا إلي ألمونيا تساوي

1500 بناء عل تجارب أجريت على العامل الحفاز في مفاعل مثبت عند درجات حرارة تتراوح من 250-400 درجة مئوية. أستخدم برنامج MATLAB نموذج قانون القوة لتقدير المعاملات الحركية.

CHAPTER 1

INTRODUCTION

1.1 Background

Propylene is one of the crucial components used in petrochemical industry to produce many chemical intermediates and polymers such as polypropylene (polypropylene accounts for more than the half of propylene consumption), oxo alcohols, propylene oxide, cumene , methyl methacrylate, phenol, acrylic acid, acrylonitrile, oligomers and many other products and intermediates. These derivatives are used in many applications such as construction, automotive, electronics and packaging [1][2][3].

Figure 1 below shows the percentages of propylene demand by its end products in 2013 where the total propylene production was 83.6 Million Metric Tons [4].

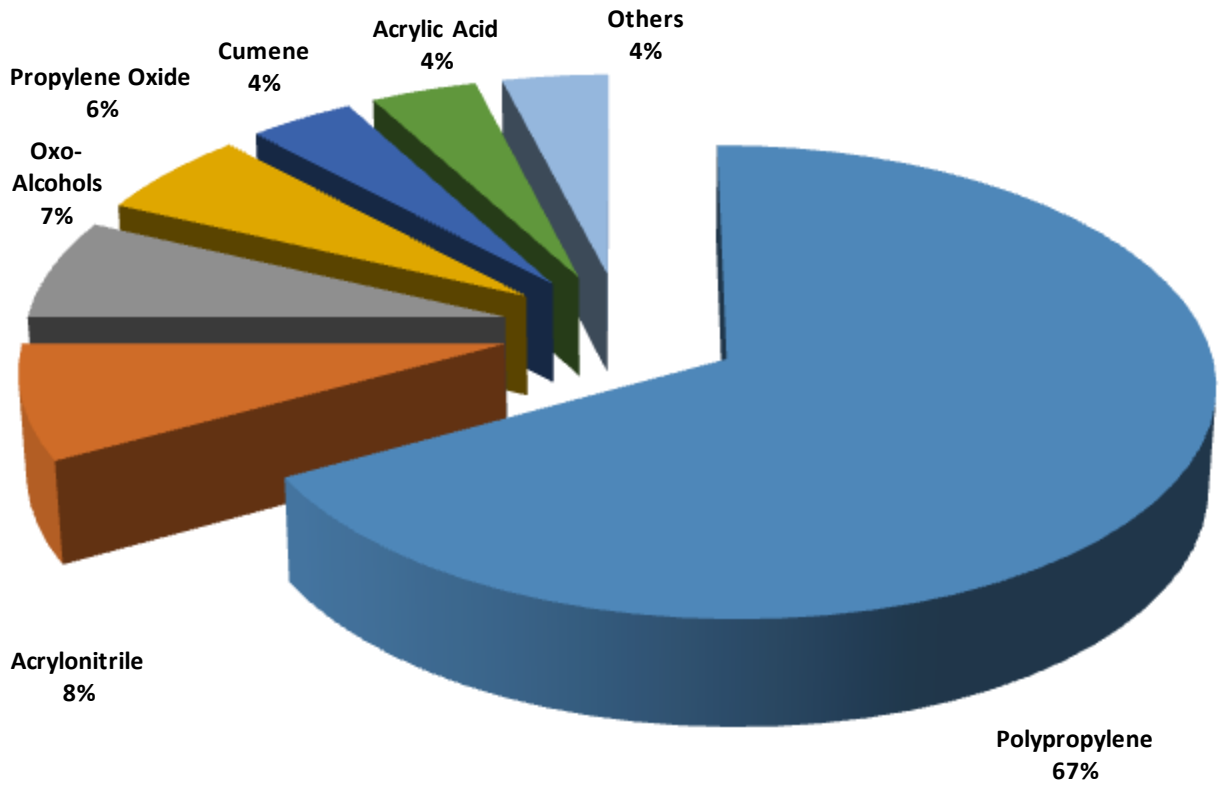

Figure 1 Propylene demand percentages by its end products in 2013 [4]

Globally, propylene demand between 1995 and 2000 increased from 37.2 million tons to 52 million tons at average annual growth rate above 5.5%, and it continued on increasing between 2000 and 2006 at an AAGR of 4.6 % to reach 67 million tons at 2006. The demand is now over to 90 million tons by 2016 [2][5].

The future demand is expected to increase at AAGR of 2.9% between 2016 and 2025, which indicates that the demand will extend to 132 million tons in 2025 [6].

In 2002, the propylene demand was met mainly by Steam Crackers Plants for ethylene production which made about 68% of total propylene production and Refinery Fluid Catalytic Cracking Units (FCC) which made 23% of total propylene production, in both sources propylene is produced as a co-product. Whereas propane dehydrogenation (PDH) and olefin metathesis made 3% of the total propylene production forming part of 'On purpose propylene production' techniques. Higher hydrocarbons catalytic cracking and methanol to propylene (MTP) and olefin interconversion are still arising [3].

The propylene demand is increasing as the need for propylene derivatives is growing, and many regions around the world have changed the feedstock of ethylene steam crackers from naphtha to lighter feedstock (ethane or LPG) due to the emergence of shale gas and shale oil, thus the supply of propylene from steam crackers has decreased as the propylene selectivity decreases with decreasing the molecular weight of the feedstock. On the other hand the supply from refinery FCC can be increased slightly; however this increment will not be adequate to meet the increasing demand for propylene. Hence, on purpose propylene supply will be needed in order to meet the shortages in demand. Although lower oil prices has made naphtha more competitive to lighter feedstock but still not affected the need for on-purpose propylene technologies. Figure 2

shows the propylene value chain from conventional sources and on-purpose propylene sources [5].

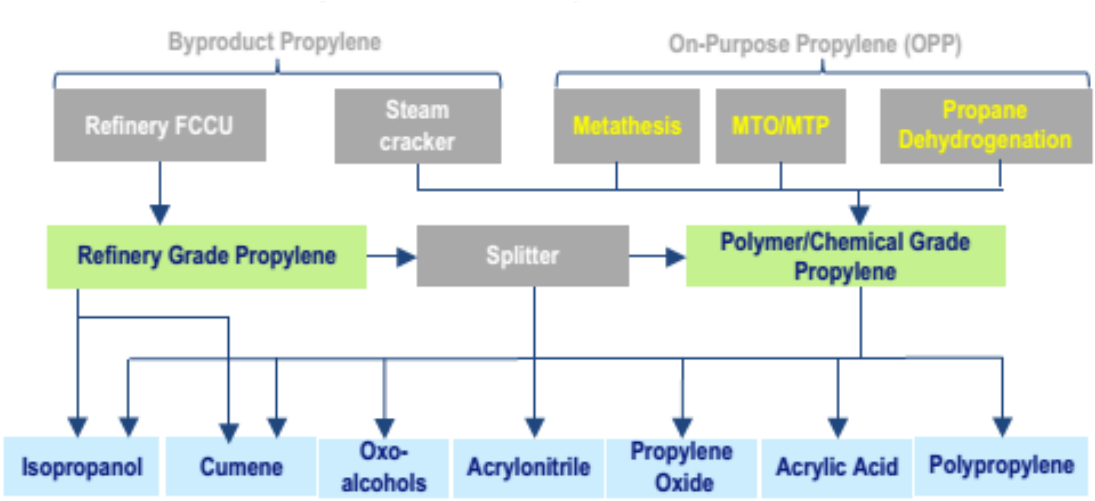

Figure 2 Propylene Value Chain [5]

Since the petroleum refining plants and ethylene production plants are growing, large amounts of C4 are produced as by-products with low value. Hence, processes like C4 alkenes catalytic cracking to produce propylene and metathesis of ethylene and butenes to propylene are becoming more attractive to explore in order to lessen the propylene demand [7].

1.2 Technologies for propylene production

Most of the propylene available is generated as a co-product from steam crackers and FCC units, so its production is driven by the need of ethylene from steam crackers and gasoline from FCC units. Also it can be produced from on-purpose propylene technologies such as: propane dehydrogenation (PDH), metathesis, methanol to olefin (MTO), methanol to propylene (MTP) and olefins cracking (C4 to C8 olefins). Figure 3 shows regional propylene supply sources in 2013 and figure 4 shows global propylene supply sources since 1990 and the forecast for 2020 [8].

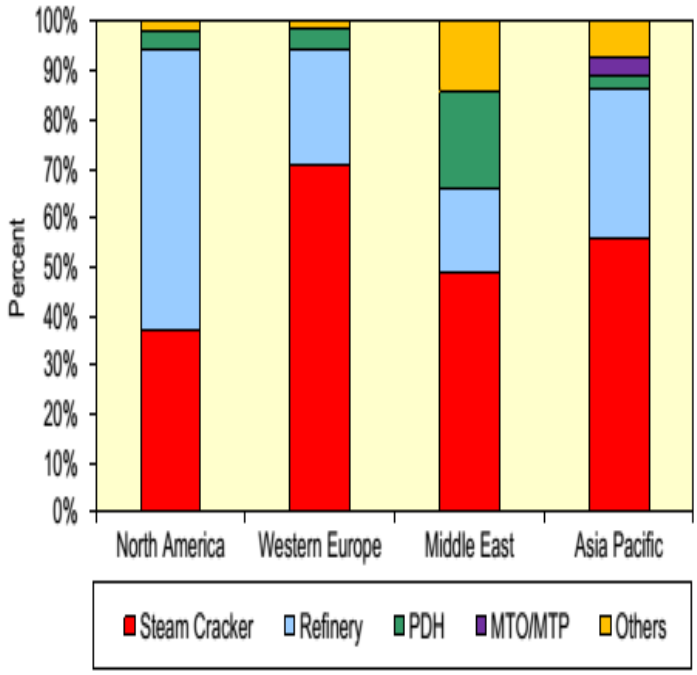

Figure 3 Regional propylene supply sources in 2013 [5]

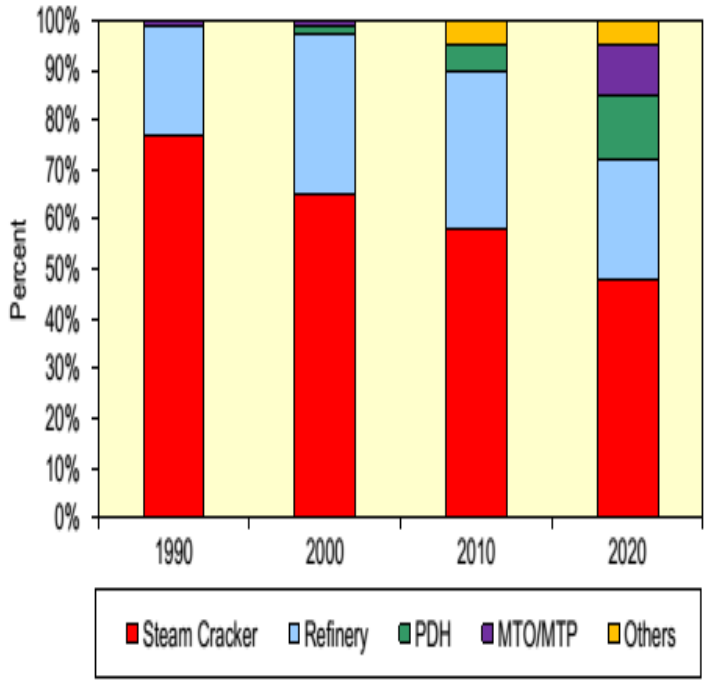

Figure 4 Global propylene supply sources [5]

1.2.1 Hydrocarbons Steam Cracking

The main technology for the production of either ethylene or propylene (light olefins), is by hydrocarbon steam cracking. This technology was used commercially for the first time in 1950s. Two main factors affect the distribution of co-products: feedstock type and the conditions of operation [2][3].

The dominant feedstocks for hydrocarbon steam crackers are ethane, LPG (Liquefied Petroleum Gas), natural gas liquids (NGLs) and naphtha (a mixture of hydrocarbons in liquid form that is produced in the oil refinery by distillation of crude oil). Steam crackers are designed to crack a single feedstock (like ethane) or a combination of feedstocks ranging from ethane to vacuum gasoil (VGO). The heavy liquid feedstocks produce a larger proportion and greater variety of by-products than lighter feedstocks [9].

Steam cracking reactions are highly endothermic (require large amounts of energy) in order to break bonds to push the reaction towards light olefins production. Superheated steam is used to lower the hydrocarbons partial pressures. It also reduces coke formation during pyrolysis at high temperature. Normal operating conditions for ethane steam cracker are 750-800^{o}C and 1.0-1.2 atm and steam flow rate is half that for ethane. Heavy hydrocarbons crack easily when compared to light ones and hence require lower temperatures to crack.

For steam cracking unit, the hydrocarbon and steam (which is used as diluent) are fed to identical cracking furnaces. The gases produced are sent to a separator (demethanizer) to separate hydrogen and methane from other gases which are treated further more to acquire acetylene, ethylene, ethane, propylene and other olefins. Liquid feeds give a wide range of products including Benzene, Toluene and Xylene (BTX). In the cracking furnaces, propylene to ethylene ratio is bounded to about 0.65, and if this ratio is increased then the total ethylene and propylene yield will drop to undesirable levels. Table 1 shows the yield of propylene in a typical steam cracker using different feedstocks and the large increase of C5+ products with heavy feedstocks [3].

Table 1 The yield of products in a typical steam cracker using different feedstocks [3]

Product yield (weight percentage on unit)	Gaseous feeds			Liquid feeds	
	Ethane	Propane	Butanes	Naphtha	Gas oil
Hydrogen and methane	13	28	24	26	23
Ethylene	80	45	37	30	25
Propylene	1.11	14.0	16.4	14.1	14.4
Butadiene	1.4	2	2	4.5	5
Mixed butenes	1.6	1	6.4	8	6
C_5+	1.6	9	12.6	18.5	32
Propylene/ethylene (weight ratio)	0.03	0.3	0.5	0.4	0.6
Propylene (weight percentage of C_3)	86.7	58.3	99.0	98.3	96.7

The steam crackers produces a propane/propylene mix that is fed into a splitter to separate purified propylene from the propane. The grade of the purified propylene can be either chemical grade or polymer grade depending on the design of the splitter. Once built the stream cracker cannot produce higher purity propylene than that for which it was designed.

A smaller degree of production flexibility is through variation of cracking severity, which is a function of operating conditions. Lower severity yields less ethylene and relatively more by-products (e.g. propylene) [9].

1.2.2 Refinery Fluid Catalytic Cracking (FCC)

FCC is utilized to crack large molecules found in vacuum gas oil down to naphtha-size molecules needed for gasoline production. Some molecules are over-cracked to a scale shorter than that required for gasoline production, including about 5% propylene [10]. 60% of the propylene generated in FCC units is utilized in the petrochemical industry while the rest is directed towards the production of blends used to increase the gasoline octane number through a process called alkylation. In alkylation, propylene is reacted with isobutane to give a highly branched, seven-carbon paraffinic mixture called alkylate. Alkylate, because it is highly branched, has good octane and is often used as a blend stock in gasoline formulation [3][10].

Figure 5 shows a flow diagram of an exemplary FCC unit. The FCC unit contains a system for injecting the feed, a reactor with the feed flowing upwards (riser), stripper, fractionator and regeneration unit. The coke formed on catalyst is burned in the regenerator and the heat produced balances the heat required by the cracking reactions which are endothermic. To ease the heat transfer between the regenerator and the reactor a fluidized catalyst is used.

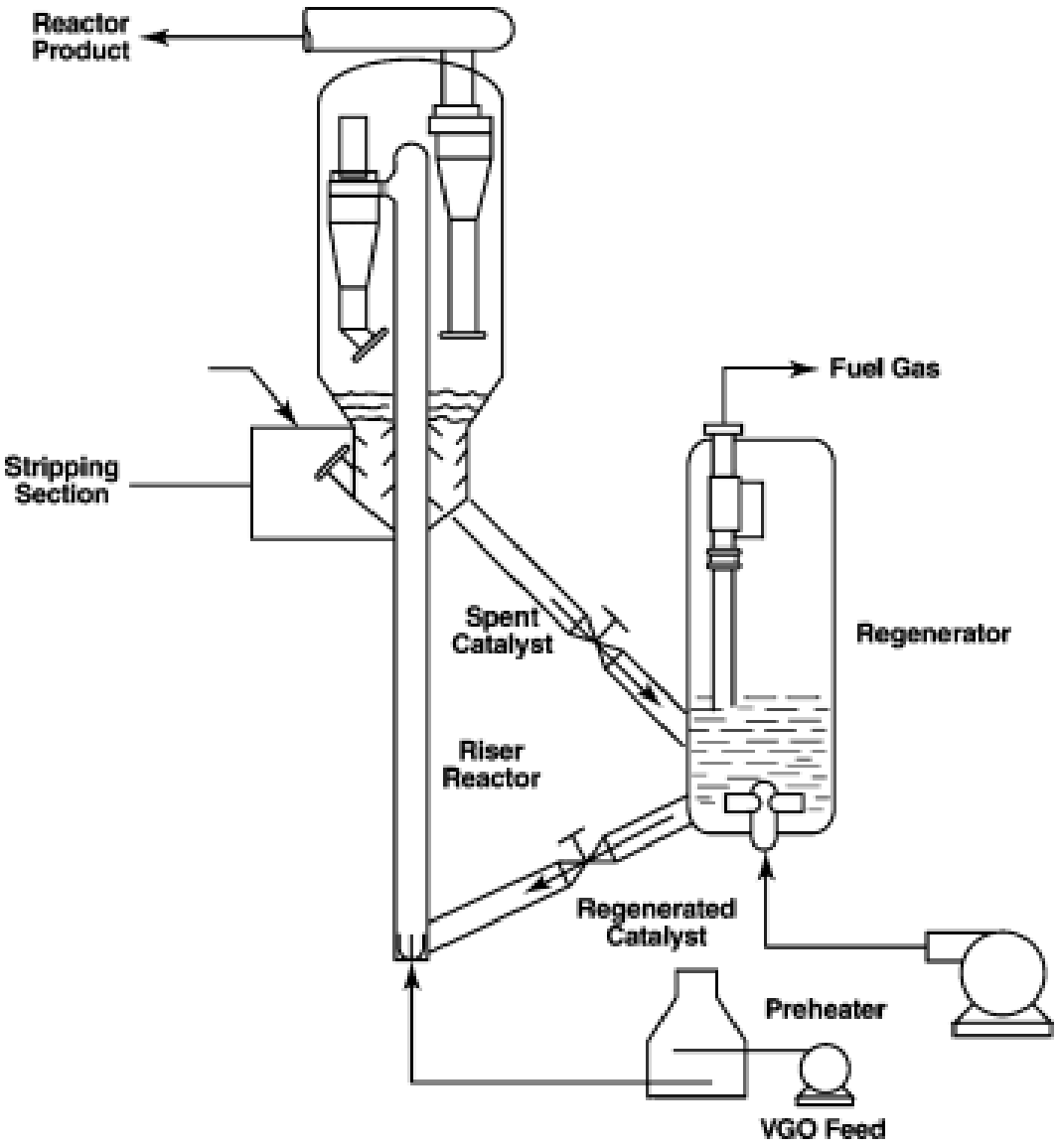

Figure 5 Flow Diagram of a Typical FCC Unit [3]

The yield of propylene from FCC unit depends on:

- The FCC unit processing capacity.
- Feedstock type.
- Riser outlet temperature.

Propylene yields also can be increased intentionally by specially formulated zeolites to the FCC catalyst, so-called enhanced FCC. Thus, the refiner is constantly keeping an eye on the value of octane versus the price of chemical-grade or polymer-grade propylene in order to ascertain where to place this refinery grade propylene to maximize margins [10]. Table 2 shows product yields from typical FCC units and other high olefin production technologies.

These two conventional sources (steam cracking and FCC) are in shortages to meet the growing propylene demand, so the following on-purpose propylene technologies (their only aim is to produce propylene) are considered.

Table 2 Product yield from typical FCC unit and emerging technologies [3]

Parameters	FCC	Deep Catalytic Cracking (DCC)	PetroFCC	High Severity-FCC
Reaction temperature (^{0}C)	500	530	590	600
Product yield (weight Percent)				
Ethylene	1.5	5.4	6.0	2.3
Propylene	4.8	14.3	22.0	15.9
Mixed butanes	6.9	14.7	14.0	17.4
Gasoline	51.5	39.0	28.0	37.8
Heavy and light oils	21.0	15.6	14.5	9.9
Coke	4.5	4.3	5.5	6.5

1.2.3 Propane Dehydrogenation

Propane is produced either by natural gas processing or by petroleum refining. Propane dehydrogenation is a catalytic process where propane is converted into propylene by the removal of hydrogen with propylene yield of 85%, while hydrogen produced as a by-product is used as a fuel for the dehydrogenation process [8]. The economics of this process depend on the availability of feedstock (propane) and cost. The availability of inexpensive propane from the shale gas in the United States will lead to many investments in propane dehydrogenation plants in that region. Figure 6 shows propane dehydrogenation flow diagram.

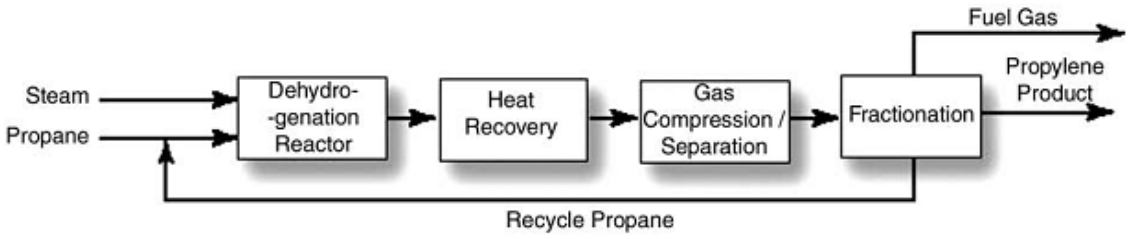

Figure 6 Propane dehydrogenation schematic flow diagram [3]

1.2.4 Methanol to Olefin/ Methanol to Propylene

Currently ethylene and propylene markets exceed that of methanol, and hence it is attractive to convert part of the large amounts of methanol to light olefins. Two processes are available for propylene production: either methanol to olefin which is a process developed by UOP and Hydro or methanol to propylene (MTP) which is a process developed by Lurgi [3]. In these processes synthesis gas is converted into methanol (syngas is produced either from coal gasification,

steam-induced reformation of petroleum products or reformation of natural gas), then the methanol is converted into light olefins [8].

1.2.5 Metathesis

In metathesis propylene is produced by the reaction of ethylene and butenes using specific transition-metal catalysts. Metathesis can be used with steam crackers or FCC units to boost the propylene yield by transforming ethylene and cracking butenes. Many processes using metathesis are available commercially such as OCT-ABB Lumus. Figure 7 shows metathesis flow diagram [3].

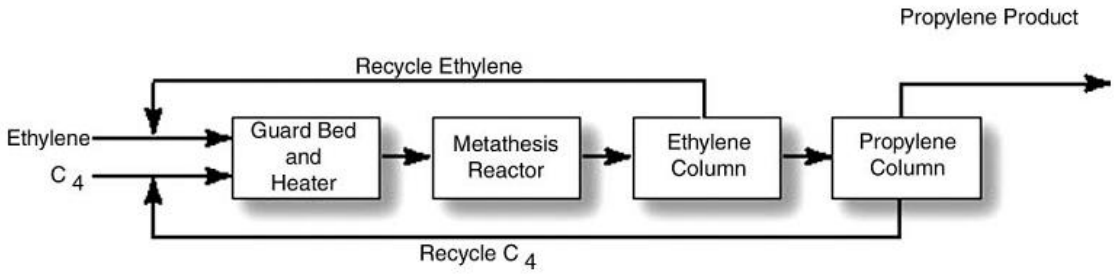

Figure 7 Metathesis flow diagram [3]

1.2.6 Olefins Cracking (Olefin Interconversion)

Propylene can be produced by cracking C_4-C_8 olefins in either fixed bed reactor or fluidized bed reactor. The process can be used in steam cracking plants or FCC units in order to enhance propylene yield. In the contrary to metathesis, cracking does not consume any ethylene but it can produce more ethylene.

The olefins cracking reactions are composed of oligomerization reactions, isomerization, cracking reactions and Hydrogen transfer reactions. The selectivity and distribution of products is determined by the catalyst and the reaction conditions. To increase propylene yield hydrogen

transfer reactions and cyclization reactions should be minimized; because these reactions lead to the formation of paraffins and aromatics.

1.3 Thesis Objectives

The main objective is to develop a new catalyst to produce propylene and ethylene from higher olefins, with a target total propylene and ethylene yield of 50 carbon wt%. The specific objectives are as follows:

1. Modify ZSM-5 type zeolites and develop a method for suppressing strong acid sites to reduce the hydrogen transfer reactions and hence form more ethylene and propylene.
2. Characterize the synthesized zeolites by XRD, BET surface area, ammonia TPD, SEM and FT-IR measurements, before and after introducing modifications in the catalyst.
3. Optimize the catalyst design to achieve higher selectivity for propylene and ethylene. Compare the catalytic activity between modified ZSM-5 type zeolites.
4. Develop reaction kinetics and elucidate the reaction mechanism for better understanding of active sites.
5. Develop novel catalyst systems with enhanced stability over 50 hours on stream.

CHAPTER 2

LITERATURE REVIEW

2.1 Introduction

Olefins cracking have been described recently by many companies, such as Exxon Mobil's Fluidized-Bed Propylene Catalytic Cracking (PCC) and Olefin Interconversion (MOI), Linde's Fixed Bed Catalytic Cracking (FBCC), SUPERFLEX technology by Kellogg Brown & Root (KBR), PROPYLUR technology by Lurgi and Olefin Cracking Process (OCP) by Atofina and UOP. The feed for such processes come from naphtha steam crackers or FCC unit. The feed preferred pretreatment is the selective hydrogenation of all dienes. Propylene yield can be increased if the dienes are converted firstly to olefins [1]. The characteristics of some olefins cracking technologies are abridged in table 3.

Table 3 Characteristics of olefins cracking processes [1]

	MOI	SUPERFLEX^{TM}	PROPYLUR	AtoFina/U
Reaction temperature	>1000 ^{0}F	900–1300 ^{0}F	≥930 ^{0}F	500–600 ^{0}C
Catalyst	ZSM-5	Zeolite	Zeolite	Zeolite
Reaction pressure	15–30 psig	1–2 bars	1.3–2 bars	1–5 bars
Reactor system	Fluid bed	Riser	Fixed bed	Fixed bed
Catalyst regeneration	Continuous, fluid bed	Continuous	Cycle	Cycle
Feed pretreatment	Selective hydrogenation of dienes	Selective hydrogenation of dienes	N/A	N/A

2.2 Basic Chemistry of Catalytic Cracking

Cracking is one of the significant reactions in the petroleum refining and the petrochemical industries. Cracking is one of the hydrocarbon reactions that are catalyzed by acid catalysts (zeolites are the most used type), the scheme in figure 8 below shows the main reactions for acid catalyzed reactions.

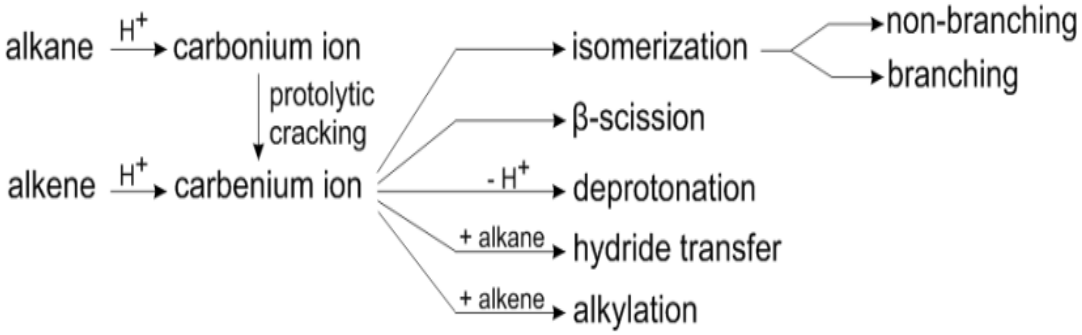

Figure 8 Scheme of the main reactions involved in alkene catalytic cracking

From the figure it can be seen that alkane protonation will yield a carbonium ion, which can be cracked protolytically to form carbenium ion, while alkene protonation will yield carbenium ion directly. Figure 9 shows the difference between carbonium and carbenium ions. These carbocations go through further reactions such as isomerization, β-scission, deprotonation, hydride transfer and alkylation.

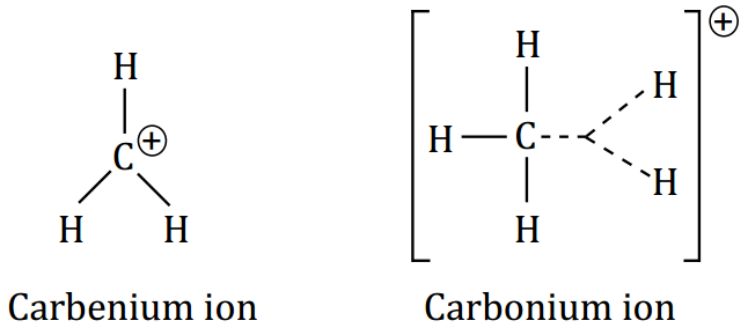

Figure 9 Carbenium ion and Carbonium ion [11]

There is a wide agreement that alkene cracking occurs on Brønsted acid sites. Firstly, the alkene physisorption occurs, where alkene is oriented with its π-electron cloud towards the partially positive charged hydrogen atom, thus forming a π-complex. This step is relatively independent of the olefin structure [12]. This π-complex goes through proton transfer (from the zeolite to the alkene) to form a carbenium ion. Carbenium ions tend to either decompose or isomerize into more stable form. Hence, alkene protonation will constantly produce secondary and tertiary ions (tertiary are more stable than secondary). On the other hand primary carbenium ions will not be produced via adsorption [13].

It has been shown experimentally that acid proton is produced from the zeolite hydroxyl groups when deuterated zeolites are used, also carbenium ion formation was shown to occur [14], though these carbocations (carbonium or carbenium) are highly reactive species which result in difficult experimental observation [13].

2.2.1 Carbenium Ion

Some of the common reactions of carbenium ions include:

i. Non-branching isomerization:

Non-branching isomerizations are rearrangements while having the same number of alkyl branches. This type includes transfer of hydrogen atom at β position and transfer of β-methyl to a positively charged carbon which is essential for skeletal isomerization [11]. The rate of non-branching isomerization occurring depends on the carbocations stability.

ii. Branching isomerization:

Branching isomerization is explained by the existence of protonated cyclopropane as an intermediate. The non-branching isomerization occurs more frequently than branching isomerization due to the high activity of branching isomerization.

iii. β-Scission:

β-scission is the most significant step in the cracking reaction. It occurs at the β position of the positively charged carbon atom. As primary carbenium ions are not stable and easily transformed into secondary and tertiary carbenium ions, methane, ethane and ethylene are not formed by β-scission [11].

iv. Alkylation:

Alkenes can be added to carbenium ions through alkylation. Alkylation reactions include dimerization and oligomerization. These reactions will be directed towards the formation of the most stable carbenium ions [15].

v. Hydride transfer and protolytic cracking:

Carbenium ions can be produced from neutral molecules through hydride transfer. But the sequential hydride transfer of alkene to carbenium ion forms aromatic compounds, e.g. benzene from propylene [11]. Also carbenium ions can be produced from carbonium ions through protolytic cracking which may produce methane if the cracking occurs at terminal C-C bond. Hence, cracking through carbonium ion produces methane, ethane and hydrogen, and at low temperatures the carbenium ion produces some propane and butane [15].

vi. Deprotonation:

Alkenes can be formed through deprotonation of carbenium ion and the proton will be sent to Brønsted basic site. The sequence of protonation and deprotonation is recognized as double bond shift [15].

vii. Aromatics formation:

Alkene cracking at high temperatures is joined with aromatics formation through hydrogen transfer reactions [16].

2.3 n-Butenes Cracking Mechanism

The butene catalytic cracking include many reactions such as isomerization, oligomerization, β-scission and hydrogen transfer reaction. It is agreed that the butene cracking follows bimolecular mechanism, which means that firstly butene will be converted to octane isomers through dimerization, and then cracked to smaller molecules through β-scission [17]. Figure 10 shows the butene cracking reaction mechanism.

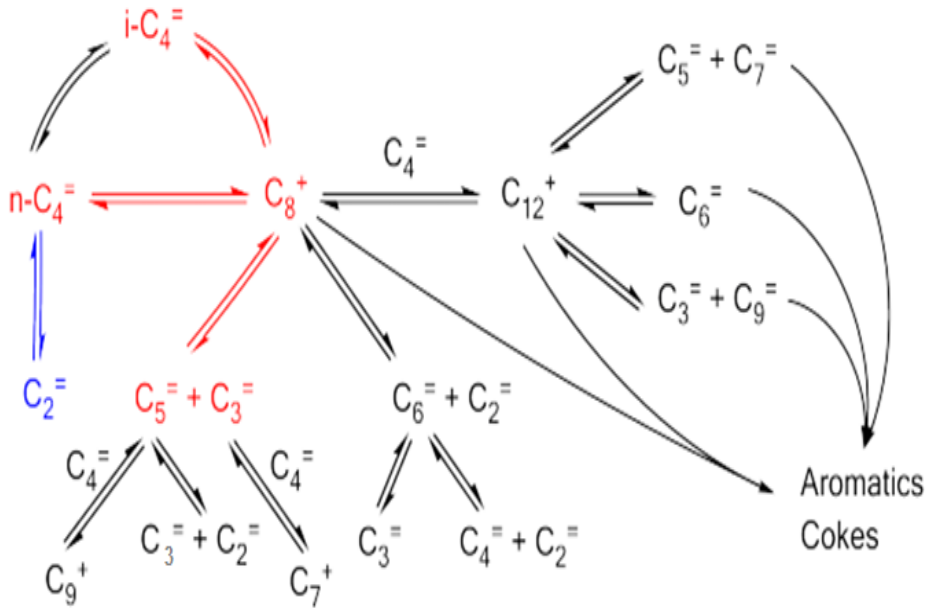

Figure 10 n-Butene cracking mechanism [18]

Octyl carbenium ions has been classified into three different forms depending on the products that they will form after cracking (C_8^I, C_8^{II} and C_8^{III}) [19]:

I. $2C_4^= \rightarrow C_8^I \rightarrow 2C_4^=$

II. $2C_4^= \rightarrow C_8^{II} \rightarrow C_2^= + C_6^=$

III. $2C_4^= \rightarrow C_8^{III} \rightarrow C_3^= + C_5^=$

These reactions have a significant effect on the propylene over ethylene ratio (P/E). Figure 11 shows 1-Butene reaction pathways along with the P/E ratio expected over ZSM-5.

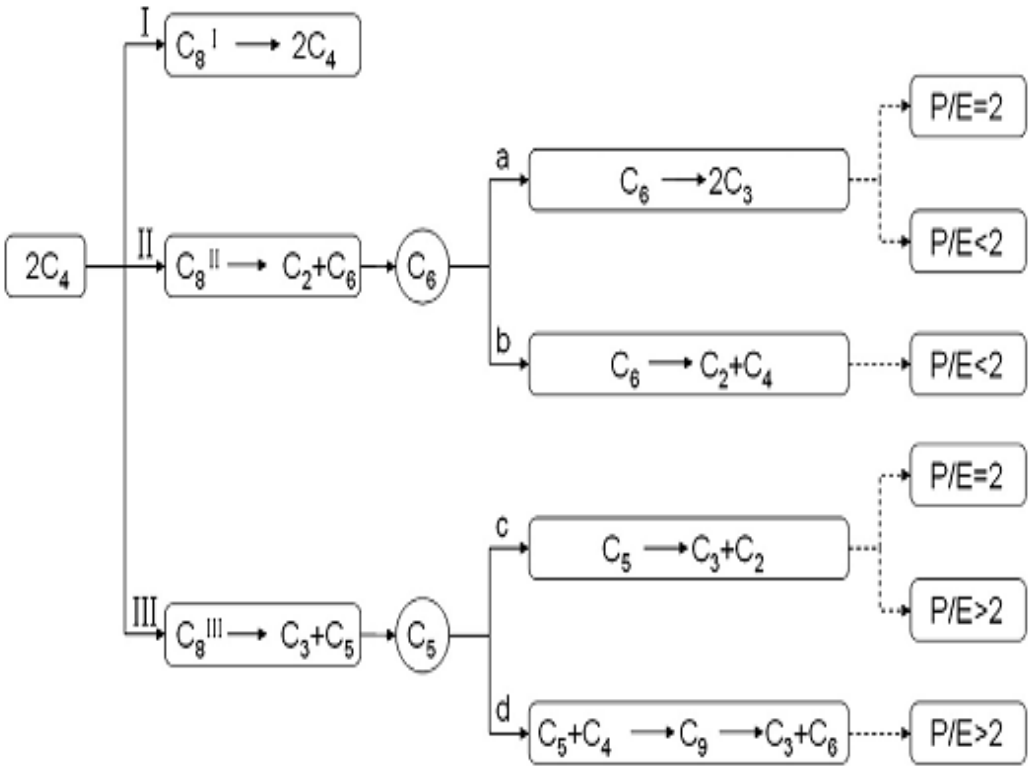

Figure 11 Reaction scheme for 1-Butene cracking over ZSM-5 to produce ethylene and propylene [19]

2.4 Cracking Catalysts

Zeolites are the most significant type of catalysts used for cracking. These are highly crystalline materials which consist of SiO_4 or AlO_4 tetrahedra with Si or Al atom at the center (termed TO_4) which gives three dimensional molecular sieve structures. Exchange of silicon atoms with trivalent aluminum atoms will result in a negative charge in the framework; which will be stabilized by cationic species which later will be exchanged by protons and hence forming Brønsted acid sites which are considered as the sites responsible of catalytic cracking.

One of the main advantages of zeolites is its unusual selectivity made by its channels and pores. Shape selectivity can be one of three types; either product shape selectivity, reactant shape

selectivity or transition state shape selectivity. Another advantage is the aluminium atom tuning which offers a wide range of zeolites acidity and density. On the other hand one of the important disadvantages of the zeolites is the coke formation.

Zeolite Socony Mobil-5 (ZSM-5) with MFI framework is one of the most used zeolites in cracking processes. It consists of a channel that is straight but has slightly elliptical opening (0.51 × 0.55 nm) intersecting with zig-zags channel that have circular openings (0.54 × 0.56 nm). Both pore types have ten membered oxygen rings [20]. Figure 12 shows the ZSM-5 structure.

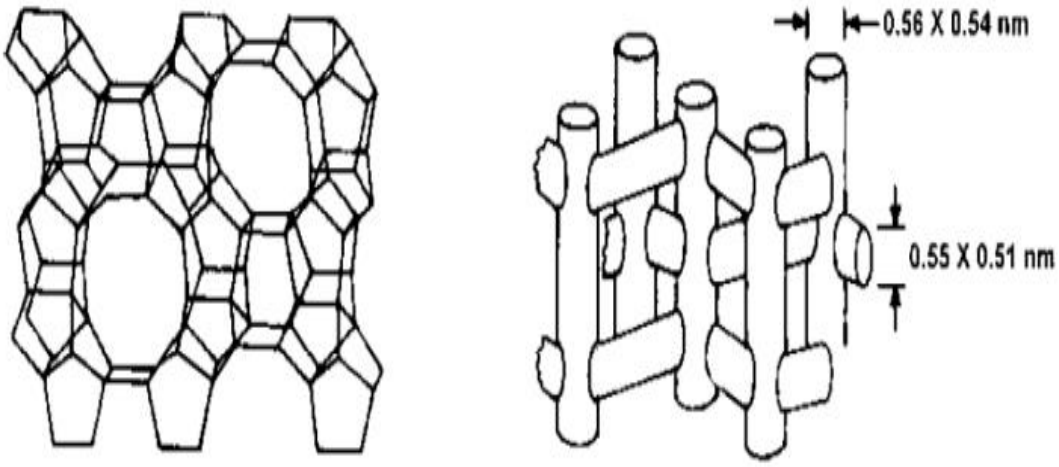

Figure 12 ZSM-5 along 100 plane (left) and Chanel dimensions (right) [20]

2.5 Effect of Zeolite Properties

Xiangxue Zhu et al. [21] investigated a number of zeolites "Y, Beta, MCM-22, ZSM-5 (Si/Al =50), ZSM-22, ZSM-23, ZSM-35 and SAPO-34" for catalytic cracking of C_4 olefins to produce propylene and ethylene, it was found that the zeolite pore structure and zeolite acidity have significant effect on the cracking performance and product distribution. NH_3-TPD was used to determine the acidity and their order from high acid sites amount to low acid sites amount is: "Y > ZSM-35 ≈ SAPO-34 > Beta ≈ MCM-22 > ZSM-5 > ZSM-23 > ZSM-22". "Zeolites of Y, Beta, MCM-22, ZSM-5, ZSM-35, SAPO-34 and ZSM-23 all possessed a large number of strong acid sites". Whereas their order for pore diameter from large pore diameters to small ones is: "Y > Beta > MCM-22 > ZSM-5 > ZSM-22 > ZSM-23 ≈ ZSM-35 > SAPO-34. Furthermore, Y and MCM-22 zeolites have large supercages in the channel systems" [21].

2.5.1 Pore Structure Effect

Butene cracking is a complex process that yields different types products. Figure 13 shows the butene conversion along with product distribution for the different types of zeolites mentioned above.

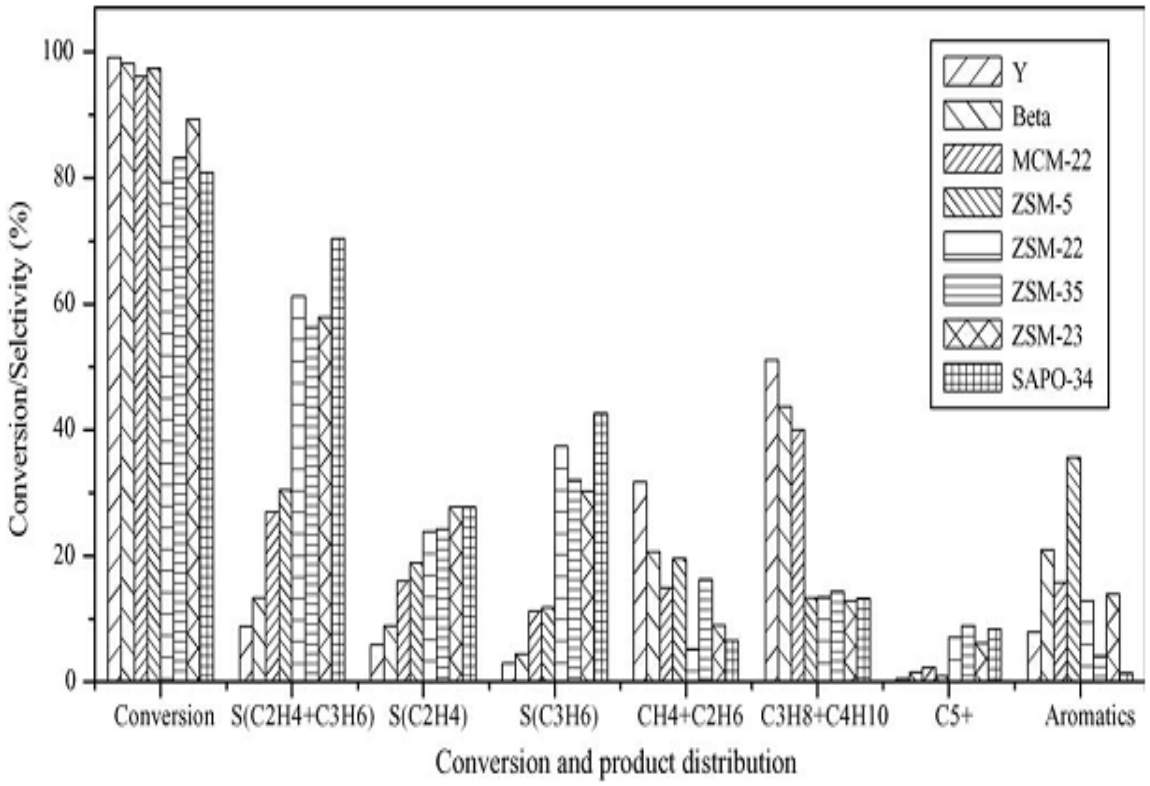

Figure 13 Conversion and selectivity of 1- butene over different zeolite structures at 620 0C, 1 bar, 3.5 WHSV and 2 minutes time-on-stream [21]

The best conversions (above 95%) were achieved by Y, Beta, MCM-22 and ZSM-5 because of their large pore diameters and high acid sites amounts. Although ZSM-35 and SAPO-34 have high acid amount, their small pore diameters hindered the reactants mass transfer and hence lowering the conversion to 83% [21].

The product selectivity was more reliant on pore structure than the conversion. Ethylene and propylene selectivity increased with decreasing pore diameter. Whereas for methane and ethane selectivity was related proportionally to the acid strength as they are produced by protolytic cracking and aromatics dealkylation. Both these reactions were favored on strong acid sites

except for SAPO-34 where the small pores quenched the production of aromatics precursors. Y-zeolite and MCM-22 large supercages induced the production of aromatics which lead coke formation [21].

Stability is one of the important factors for assessing the catalyst performance along with the activity and the selectivity. Y-zeolite, ZSM-22, ZSM-35 and SAPO-34 conversions fell down to lower than 20% after the first hour and hence showing very poor stability. The stability test for the other four catalysts is shown in figure 14.

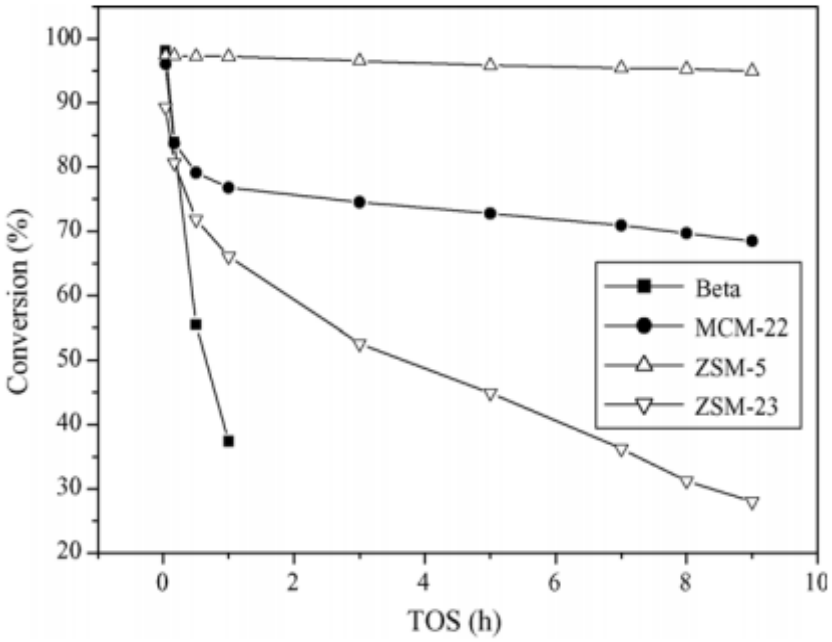

Figure 14 Stability test for Beta, MCM-22, ZSM-5 and ZSM-23 over 9 hours TOS [21]

From figure 14 it is obvious that ZSM-5 is the most stable catalyst among all the eight tested catalyst and this is due to its 10 membered oxygen ring which hinders the formation of coke. Moreover, its intersection between the channels lowers the probability of pore blocking [21].

Form the above ZSM-5 is the most appropriate zeolite for butene cracking among the tested catalysts because of its high activity, selectivity and stability.

2.5.2 Acid Site Density Effect

Since ZSM-5 was found to have the best pore structure for butene cracking, it was investigated to elucidate the effect of the acidity on the product distribution. Figure 15 shows 1-butene conversion along with ethylene, propylene and aromatics yield for different Si/Al ratios.

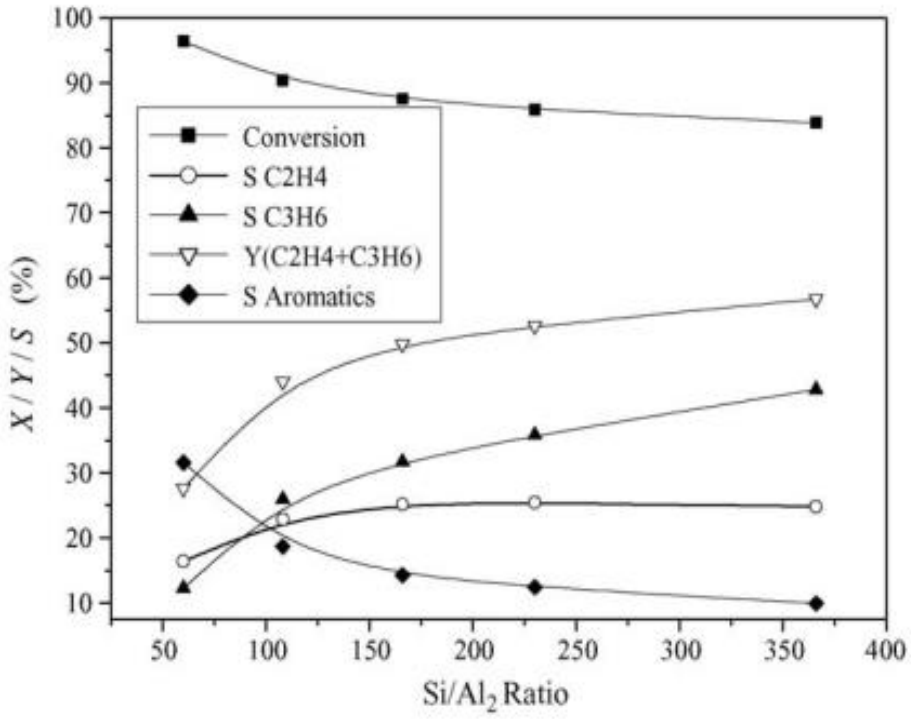

Figure 15 1-Butene conversion and products yield over ZSM-5 with different Si/Al ratios [21]

Propylene and ethylene selectivity increases with increasing Si/Al ratio, whereas the aromatics yield decreases with increasing Si/Al and hence less coke will be formed with increasing Si/Al ratio [21]. So, the increase in Si/Al ratio will reduce the acidity of the catalyst and hence reduce side reactions (hydrogen transfer reaction) which yield aromatics and alkanes [22].

Further Studies has been done on zeolites including modifications on ZSM-5 in order to enhance activity, propylene selectivity and hydrothermal stability. Phosphorous has been used in several

studies. Phosphorous and HNO_3 have been used to modify ZSM-5 as in the study carried out by Lin et al. [19]. They studied the effect of the acid strength on propylene selectivity. They found that HNO_3 and phosphorous reduced the strong acidity on the catalyst which increased the propylene selectivity, hence the catalytic performance can be controlled by controlling the distribution of acid strength. Eplede et al. [23] used K and P to modify ZSM-5 which increased the yield of propylene. They suggested that treatment with 'K' affected the distribution of acid strength and led to higher propylene yield by inhibiting the side reactions of hydrogen transfer and aromatization. The catalyst stability is enhanced due to reduction in coke formation reactions. Li et al. [24] used Fe to modify P-ZSM-5 and studied the effect of this modification on the catalyst acidity, it is found that Fe addition resulted in slight change on the catalyst acidity. However, iron addition led to increased surface area and basicity (which suppress hydrogen transfer reactions) on the catalyst, so the iron addition caused higher propylene selectivity.

Other phosphorous modification was done on HITQ-13 zeolites by Zeng et al. [25]. The surface area, crystallinity and the volume of the pores of PITQ-13 was reduced when compared to the HITQ-13. The acid strength distribution was changed with decreasing the number of sites with strong acidity and increasing the number of sites with weak acidity. When using 1.0 wt% P in PITQ-13-2 the propylene yield is 41.5% and the ethylene yield is 15.7%, but information about stability is not available.

Palani et al. [26] reported that silicate-1 is an efficient catalyst for propylene production from 1-butene due to the absence of sites with strong acidity and the presence of sites with weak acidity. It is assumed that the sites with weak acidity are the silanol groups (Brønsted sites) above 300^oC, but it is still not known which type of silanol group is responsible for the cracking. The yield of

alkenes other than n-butenes is 60 C-wt% and 34.1 C-wt% propylene yiled at 550^{o}C over silicate-1.

The foregoing discussions show that there has been no report on the utilization of surface modification such as the silica deposition using chemical liquid deposition method or core-shell silicalite composite synthesis using the hydrothermal method as modification for ZSM-5 as cracking catalyst for producing ethylene and propylene (light olefins) from the catalytic cracking of 1-butene.

CHAPTER 3

EXPERIMENTAL METHODOLOGY

3.1 Experimental Setup

The experimental setup of the reaction system for the testing of the catalyst activity consists of fixed bed tubular reactor system, the gas chromatographic system and its calibration:

3.1.1 Fixed Bed Tubular Reactor System

The reaction system is a complete reaction microsystem for the evaluation of the catalyst while analyzing the data in continuous flow process. Up to six inputs can be handled in the reactant preparation section; two of these inputs are liquid pumps with high pressure and the other four are mass flow controllers. The reactants are mixed and vaporized to create a non-fluctuating homogeneous stream which is then sent to the reactor.

Before sending the feed to the system; its flow is controlled with valves, filters, thermal mass flow controller and a 2 or 3-way diverter valve.

Fixed bed tubular reactor along with a thermostat and a tube furnace heater are provided. The temperature in the heater and the reactor are controlled with two thermocouples, these are placed in an isothermal oven. This oven is heated using a forced convection blower to ensure unwanted condensation is reduced. The valve of the type multi-port allows the reactant bypass around the reactor; this gives an appropriate method of conducting analysis for the material coming directly from the feed. Putting the reactor on the "by-pass" mode, the reactor contents will be ejected to a safe outlet.

Mechanical gauge and digital pressure transducer are used to measure pressure at the reactor inlet. The gauge and the transducer are insulated with an isolator filled with silicone with a stainless steel sheet welded to the isolator. Back pressure controller is used to maintain the pressure. Pressure digital indication is also provided.

The gaseous products coming out of the reactor are transferred to a GC through a heated transfer line. This transfer is controlled with a heated multi-port sampling valve which is placed inside the isothermal oven.

Three adjustable PID controllers are part of the system control; they are used to control the temperature of the reactor, the temperature of the oven and the temperature of the transfer line. Also the multi-port reactor status and the sampling valves are allowed to rotate. The risk of hazardous over pressurization is eliminated by using a rupture disk. The multi-port reactor status valve permits the reactor purging throughout shutdown. Some individual temperature controllers allow power termination to any heater controlled by a sensor. The above-mentioned setup is shown in Figure 16.

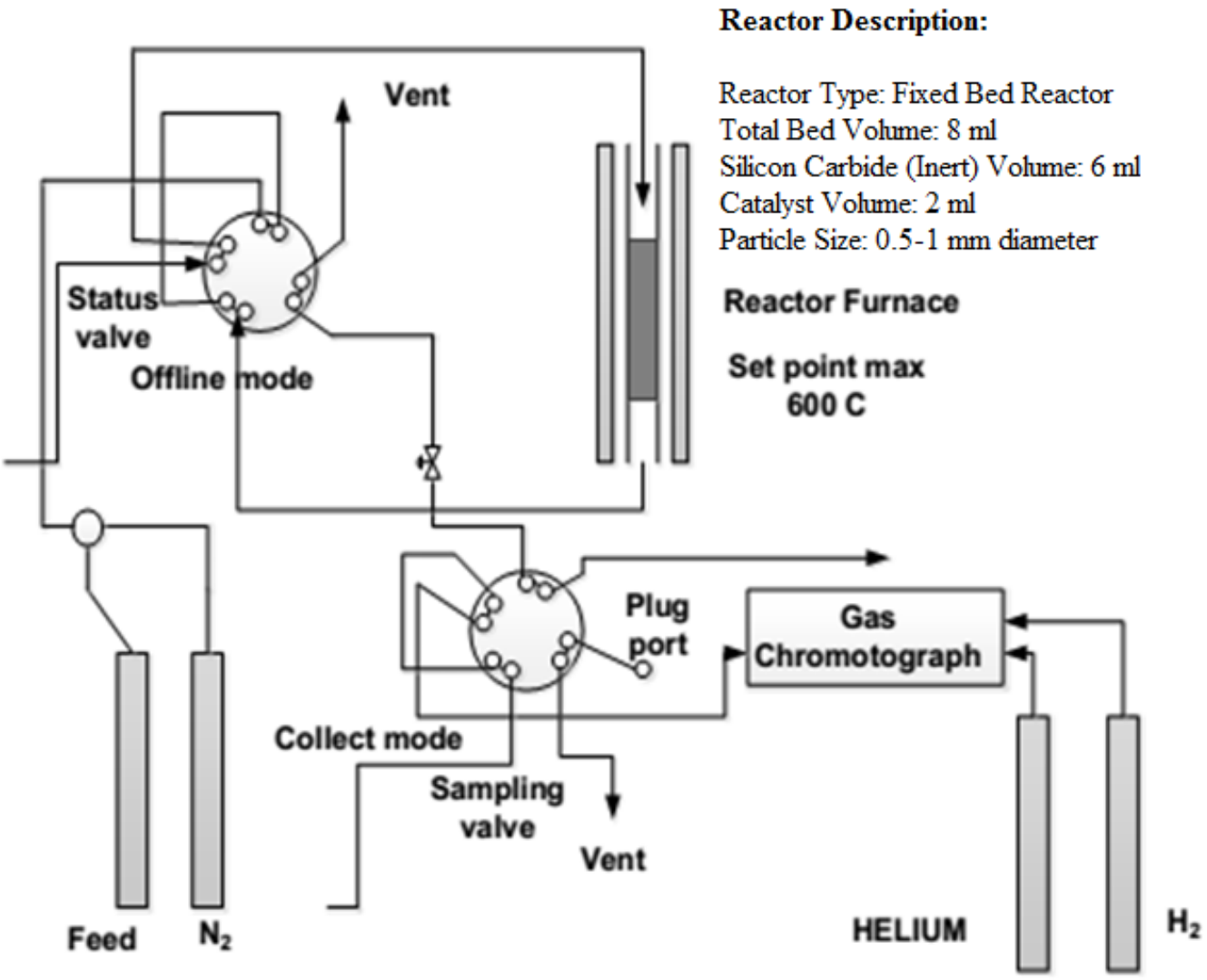

Figure 16 Schematic diagram of the fixed bed tubular reactor

3.1.2 Gas Chromatographic (GC) system

Analyzing the products of the reaction quantitatively was conducted through the use of Varian Gas Chromatograph (Varian 450-GC) equipped with Flame Ionized Detector (FID). The FID has a column of CP-Al_2O_3/Na_2SO_4 with length of 50 m, the internal diameter (I.D.) of the column is 0.32 mm and the film diameter (df) is 5µm. The GC was programmed from 50 to 100 ^{0}C at a rate of heating of 8 ^{0}C/min (hold it for 10 min at 100 °C) and 100 to 250 °C at a rate of 10 °C/min (hold it for 5 min at 250 °C). The carrier gas used is Helium (He), whereas hydrogen and air are used in the Flame Ionized Detector (FID). Moreover, Nitrogen in the liquid state is utilized to ease the beginning of the cryogenic running of the temperature programming for the Gas Chromatograph. The temperature of the Gas Chromatograph can be lowered to -30^{0}C using liquid nitrogen. A solenoid valve controls the liquid nitrogen flow actuated from the controller of the internal temperature of the Gas Chromatograph oven. The integrator permits recording of strip chart in addition to the integration of the signal of the Gas Chromatograph detector.

3.1.3 Gas Chromatographic (GC) Calibration

The GC Calibration was done to determine the distribution of the reaction products as follows:

i. Retention Time determination of the compounds:

Analysis of the pure sample of the specific compounds using the GC allows the determination of the retention times which are used to differentiate between the components in the reaction effluent stream. These hydrocarbons along with their corresponding retention times are shown in table 4. While table 5 shows the same information for the different aromatics.

Table 4 Retention time of different hydrocarbons in the GC

Compounds	Retention time (min)
Methane	1.79
Ethane	2.43
Ethylene	2.83
Propane	4.91
Propylene	7.60
I-Butane	9.39
n-Butane	10.18
1-Butene	13.63
Isobutylene	15.31
t-2-butene	15.55
cis-2-Butene	15.88
I-Pentane	16.00
n-Pentane	16.69
3-Methyl-1-Butene	19.45
1-pentene	20.50
t-2-Pentene	21.06
c-2-pentene	21.40
2-Methyl-1-Butene	22.64
1-hexene	23.05
2-Methyl-2-Butene	23.35
2,3 dimethyl1-butene	23.42
t-3-hexene	23.56
cis-3-hexene	24.22

Table 5 Retention time of different aromatics in the GC

Compounds	Retention time (min)
Benzene	4.71
Toluene	6.62
Ethyl benzene	8.65
m-Xylene	8.85
p-Xylene	9.02
o-Xylene	9.83
Isopropyl benzene	10.17
n-propyl benzene	10.77
1-Methyl-3-ethylbenzene	11.15
1-Methyl-4-ethylbenzene	11.21
1,3,5-Trimethyl benzene	11.72
1-Methyl-2-ethylbenzene	12.21
1,2,4 tri-methyl benzene	12.78
1,2,3 tri-methyl benzene	13.64
Indan	13.72
1,4 diethyl benzene	14.34
n-Butyl benzene	14.59
1,2 diethyl benzene	15.66
1,2,4,5 tetra-methyl benzene	17.02
1,2,3,5 tetra-methyl benzene	17.29
Naphthalene	21.57
Pentamethylbenzene	23.29
1-Methylnaphthalene	24.94
2-Methylnaphthalene	25.46

ii. Determination of the compound weight percentage by correlating the carbon weight percentage to the response of the GC:

For the calibration of the Gas Chromatograph, standardized samples with variant compositions comprised of the feed (1-butene) and the major components in the effluent stream (ethylene, propylene, 2-butene, pentene, hexene) were provided. The calibration injections of the samples used were of 0.2µl provided to the Gas Chromatograph. Then, the responses of the GC were obtained in area % for the different components in the variant samples used.

3.2 Experimental Method

The experimental method illustrates the various reagents used, the synthesis of the catalysts, the characterization of the catalyst using specific characterization techniques and the procedure used to perform the reaction.

3.2.1 Reagents

Tetrapropylammonium bromide (98%), anhydrous hexane (95%), tetraethyl orthosilicate (99%), ammonium fluoride (98%), fumed silica (Cab-O-sil M-5) (99.8%) were purchased from Sigma-Aldrich. 1-Butene (99.9%) was procured from Saudi Industrial Gas Company.

3.2.2 Catalyst synthesis

Ammonium form of ZSM-5 zeolites with Si/Al_2 molar ratios (23, 80 and 280) were obtained from Zeolyst International. ZSM-5 with Si/Al_2 molar ratio of 1500 was purchased from Tosoh. These parent materials were calcined at 550^{o}C for 4 h in air to convert them into H-form and denoted as catalyst A, B and C, as shown in Table 6.

Silica coating on ZSM-5 zeolites with a different SiO_2/Al_2O_3 ratio of 23, 80 and 280 was carried out using chemical liquid deposition (CLD) method [27]. Before silica coating, the zeolite materials were calcined at 550°C for 4 h at 5°C/min heating rate. In a typical coating procedure, 10 grams of parent zeolite was suspended in 100 ml of n-hexane solvent and the mixture was heated until reflux at 70°C. After 30 minutes of stirring, the TEOS solution corresponding to a loading of 4 wt% SiO_2 was added and silylation lasted for 2 h at 70°C accompanied by reflux and stirring. Then the sample was dried in a vacuum in order to remove excess n-hexane. Finally, the catalyst was dried at 100°C for 24 h and calcined at 550°C for 4 h, with a 5°C/min heating rate. After each TEOS deposition 2g of catalysts were taken from a batch and subjected to

physicochemical characterization and catalyst activity test. Silylation treatment was carried out six times using the same procedure and the samples obtained after third and sixth cycles were denoted as shown in Table 6.

Core-shell silicalite composite [28][29] was synthesized using SiO_2/Al_2O_3 ratio 280. The parent material was mixed with gel composition of 1 SiO_2: 0.08 TPABr: 0.1-2.0 NH_4F: 20 H_2O. The ratio of parent material and silica in the gel was about 1:2. ZSM-5(280)-core-shell (1X) [Catalyst C3in table 6] composite was prepared using tetra propyl ammonium bromide as structure directing agent and ammonium fluoride as mineralizer. In a typical synthesis procedure, 6g of ZSM-5 (280) zeolite was mixed well with silicalite-1 gel prepared using the following molar composition of the gel: 1 SiO_2: 0.08 TPABr: 1.6 NH_4F: 20 H_2O. The mixed gel was subjected to a hydrothermal process at 200°C for 2 days. The obtained solid sample was then washed with deionized water, filtered, dried and calcined at 550°C for 6 h.

ZSM-5(280)-core-shell (2X) [Catalyst C4 in table 6] composite was prepared using 6g of Catalyst C3 mixed well with silicalite-1 gel prepared using the following molar composition of the gel 1 SiO_2: 0.08 TPABr: 1.6 NH_4F: 20 H_2O. This was subjected to a hydrothermal process at 200°C for 2 days. The sample was then washed with deionized water, filtered, dried and calcined at 550°C for 6 h.

Table 6 List of catalysts codes used for 1-butene catalytic cracking and its description

Catalyst Code	Description
A	CBV 2314 from Zeolyst International calcined in air at 550°C for 4 hrs. SiO_2/Al_2O_3 (mol/mol) = 23.
A1	3 times silica deposition using CLD method on catalyst A
A2	6 times silica deposition using CLD method on catalyst A
B	CBV 8014 from Zeolyst International calcined in air at 550°C for 4 hrs. SiO_2/Al_2O_3 (mol/mol) = 80.
B1	3 times silica deposition using CLD method on catalyst B
B2	6 times silica deposition using CLD method on catalyst B
C	CBV 28014 from Zeolyst International calcined in air at 550°C for 4 hrs. SiO_2/Al_2O_3 (mol/mol) = 280.
C1	3 times silica deposition using CLD method on catalyst C
C2	6 times silica deposition using CLD method on catalyst C
C3	Silica deposition by core-shell synthesis using catalyst C
C4	Silica deposition by core-shell synthesis using catalyst C3
D	890HOA from TOSOH Japan, calcined in air at 550°C for 4 hrs. SiO_2/Al_2O_3 (mol/mol)=1500

3.2.3 Catalyst Characterization

The characterization techniques used are:

3.2.3.1 XRD:

The zeolite samples were characterized by X-ray powder diffraction using the system of Rigaku Mini-flex II which uses CuKα radiation filtered by nickel (λ = 1.5406 Å, 30 kV and 15 mA). The patterns of X-ray powder diffraction were obtained using the mode of static scanning starting from 1.2 - 50° (2θ) while the angular speed of the detector was 2 ° min^{-1} with the size of the step of 0.02°.

3.2.3.2 Nitrogen Adsorption Isotherm:

The surface areas of the different catalysts were measured through the use of nitrogen adsorption at -196^{o}C with Autosorb-1 (Quanta Chrome) using the equation of Brunauer Emmett-Teller (BET) while the pore diameters were calculated using Barrett-Joyner-Halenda (BJH) method.

3.2.3.3 Scanning Electron Microscopy (SEM):

For SEM images, a sample holder was used to load the catalysts on, these catalysts samples were held through the use of a tape of aluminum and covered by a diaphragm of gold in a vacuum. The gold coating was performed using ion-coater of cressington sputter type, the caoting continued for 20s using a current of 15 mA. A scanning microscope of JEOL JSM-5800 was used to capture SEM of images of the gold-coated samples, a 7000 times magnification was obtained using the SEM.

3.2.3.4 Fourier Transform Infrared Spectroscopy (FT-IR):

FT-IR analysis was performed for the catalysts in order to identify the silanol groups present in the catalysts. The thin wafer of catalyst sample was prepared and then transferred to an *in-situ* cell of the type Makuhari Rikagaku Garasu Inc., brought from Japan. This *in-situ* cell operates under vacuum for pretreatment of the catalyst samples for 1 hour under (*ca*. 2 x 10^{-1} Pa) at 450°C. All spectra measurements were performed at room temperature with Nicolet FT-IR spectrometer (Magna 500 model).

3.2.3.5 Temperature-Programmed Desorption (TPD):

TPD of ammonia was conducted using thermogravimetric analyzer (TGA). 25 mg catalyst sample was taken in a crucible and was subjected to a pretreatment at temperature of 500 ^{o}C under a flow of helium for 60 minutes. Then it was exposed to 5% ammonia in He at 100^{o}C for 15 minutes. Excess ammonia adsorbed was flushed by helium stream for 30 min at 100^{o}C. Desorption of ammonia was monitored using TGA from 100^{o}C to 600^{o}C at a ramp rate of 10°C per min.

3.2.3.6 External surface acidity Testing:

The acidity of the external surface of the catalysts was measured by cracking of 1,3,5 triisopropyl benzene (TIPB) using a fluidized-bed reactor at atmospheric pressure. Vora et al. [30] in US Patent of "Enhanced Light Olefin Production" gave a detailed description about the riser simulator. The experiments were performed with 0.81 g of catalyst and 200 µl of TIPB at 550°C for 20 s.

3.2.4 Reaction Procedure

Fixed-bed reactor was used for the evaluation of the catalytic performance of the different catalysts. The reactor is made of stainless steel tube of grade 316, the internal diameter (ID) of the tube is 0.312 inch while the outer diameter is 0.562 inch and the tube length is of 8 inches. The reactor is packed with 2 ml of the catalyst with the size of the particle diameter between 0.5 mm to 1.0 mm. A pretreatment of the sample at a temperature of 550°C with a flow of nitrogen was performed for 1 hour to activate the catalyst sample. After that, the feed was introduced to the reactor which comprised of nitrogen used as diluent and the main hydrocarbon feed 1-butene at 25 ml/min and 5 ml/min, respectively (GHSV=900h^{-1}). This stream with the mentioned composition moved through the catalyst bed at temperature of 550°C. The effluent stream coming out of the reactor was sent to an online GC for analysis. The GC is equipped with a GS-Gaspro column together with a FID detector.

In order to investigate the impact of the temperature on the selectivity of the different components in the outlet stream for some the catalysts of interest; the temperature of the reactor was changed to study the effect between 150°C to 550°C.

After obtaining the analyzed data from the GC, it was used to obtain the following as obtained from Liu et al. [31]:

Molar Conversion of 1-butene:

$$X_{(1-C_4^=)} = \frac{moles\ of\ 1-butene\ converted\ (\frac{W(1-C_4^=)}{4})}{moles\ of\ 1-butene\ fed} \times 100\%$$

Yield:

$$Yield, Y(C_n^=) = \frac{X_{(1-C_4^=)} \times \frac{W(C_n^=)}{n}}{\frac{W(C_2^=)}{2} + \frac{W(C_3^=)}{3} + \frac{W(C_4^=)}{4} + \frac{W(C_5^=)}{5} + \frac{W(C_6^=)}{6}} \times 100\%$$

In the formula, $Y(C_n^=)$ for the olefin with *n* carbons in its structure is the yield for that component, and $W(C_n^=)$ for the olefin with *n* carbons in its structure is the weight percentage for that component.

CHAPTER 4

RESLUTS AND DISCUSSION

4.1 Catalyst characterization

The catalyst characterization has been performed before and after modifying the catalyst in order to study the effect of the modification on the properties of the catalyst. The characterization techniques used are:

4.1.1 X-Ray Powder Diffraction

XRD patterns of ZSM-5 and modified ZSM-5 catalysts are presented in Figure 17 and Figure 18. All samples show the characteristic peaks of ZSM-5 structure in the ranges 2θ= 7- 10° and 22-25° as reported in the literature [32][33][34][35]. Due to the difference in crystal growth, the relative intensity of diffraction peaks was different depending on the sample. The peak at 2θ=7.9 is a superposition of the diffractions from (-1 0 1), (0 1 1) and (1 0 1) faces. The peak observed at 2θ= 8.9 is superposition of the diffraction from (0 2 0), (2 0 0), (-1 1 1) and (1 1 1) faces. The *d* spacing values for all the catalyst are presented in Table 7.

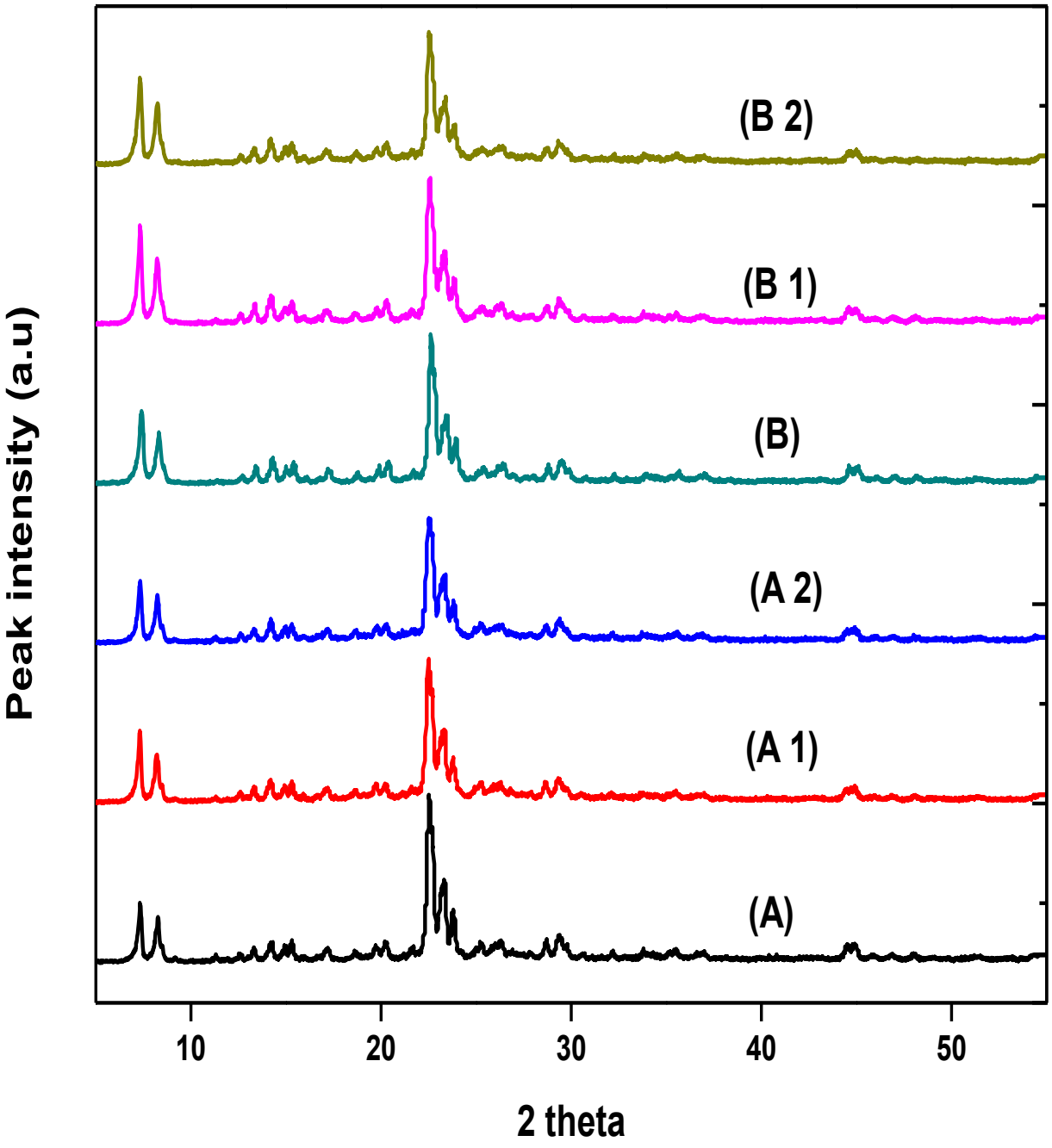

Figure 17 XRD patterns of (A) H-ZSM-5(23), (A 1) H-ZSM-5(23)-3X, (A 2) H-ZSM-5(23)-6X, (B) H-ZSM-5(80), (B 1) H-ZSM-5(80)-3X and (B 2) H-ZSM-5(80)-6X catalysts

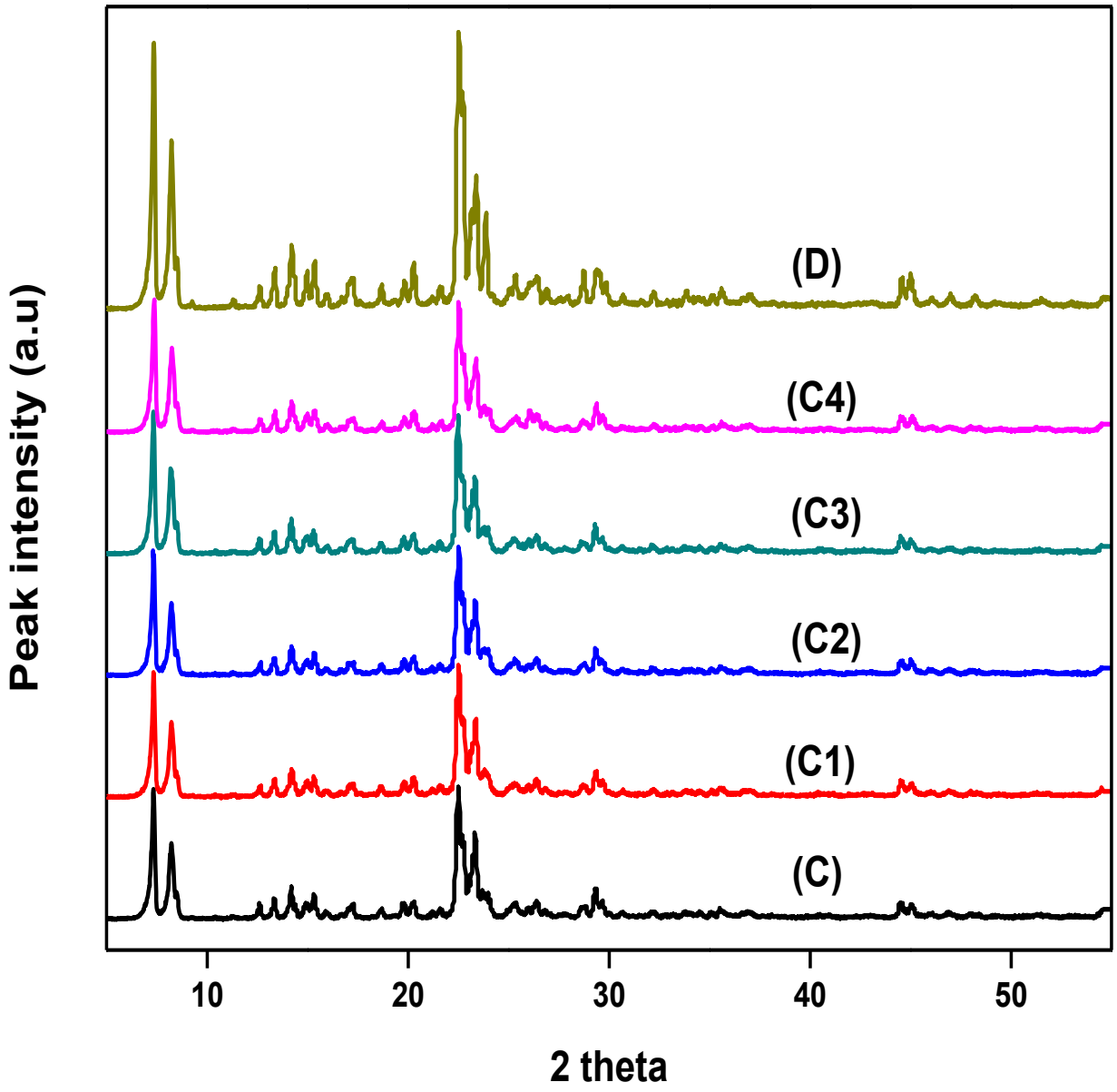

Figure 18 XRD patterns of (C) H-ZSM-5(280), (C 1) H-ZSM-5(280)-3X, (C 2) H-ZSM-5(280)-6X, (C 3) H-ZSM 5(280)@CoreShell-1X, (C 4) H-ZSM-5(280)@CoreShell-2X and (D) H-ZSM-5(1500) catalysts

Table 7 $d_{spacing}$ for the different Catalysts

Catalyst	$d_{spacing}$ (Å)
A	3.942
A1	3.948
A2	3.942
B	3.927
B1	3.936
B2	3.941
C	3.948
C1	3.948
C2	3.949
C3	3.949
C4	3.946
D	3.945

(A) H-ZSM-5(23), (A 1) H-ZSM-5(23)-3X, (A 2) H-ZSM-5(23)-6X, (B) H-ZSM-5(80), (B 1) H-ZSM-5(80)-3X, (B 2) H-ZSM-5(80)-6X, (C) H-ZSM-5(280), (C 1) H-ZSM-5(280)-3X, (C 2) H-ZSM-5(280)-6X, (C 3) H-ZSM 5(280)@CoreShell-1X, (C 4) H-ZSM-5(280)@CoreShell-2X and (D) H-ZSM-5(1500) catalysts

4.1.2 Nitrogen Adsorption Isotherm

The nitrogen adsorption isotherms for the parent as well as modified ZSM-5 samples were recorded (Figure 19 and Figure 20) and the total surface areas are presented in Table 8. These materials exhibit type IV classification, characteristic of mesoporous materials. The BET surface area was slightly decreased for catalysts ZSM-5(23)-3X (A1) and ZSM-5(23)-6X (A2) as compared to catalyst ZSM-5(23) (A). The decrease in a surface area related to continuous external surface passivation by chemical liquid deposition using tetraethylorthosilicate. A similar trend was also observed for catalyst ZSM-5(80)-3X (B1), ZSM-5(80)-6X (B2), ZSM-5(280)-3X (C1) and ZSM-5(280)-6X (C2). Upon silica deposition, the micropore volume of the catalyst was also decreased as shown in Table 8. However, catalysts ZSM-5(280)@CoreShell-1X (C3) and ZSM-5(280)@CoreShell-2X (C4), synthesized using core-shell method retained the BET surface area of parent materials.

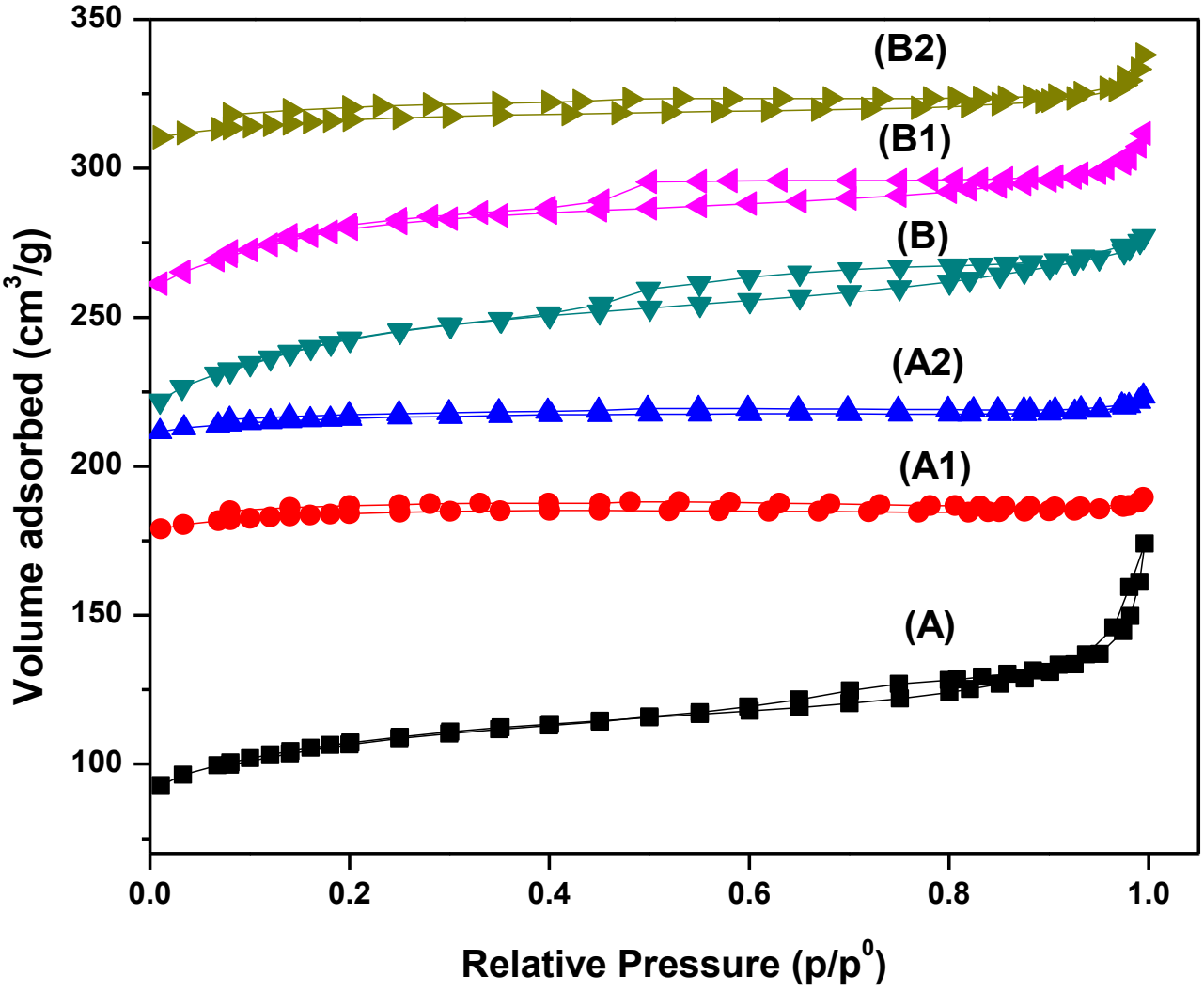

Figure 19 Nitrogen adsorption-desorption isotherms of of (A) H-ZSM-5(23), (A 1) H-ZSM-5(23)-3X, (A 2) H-ZSM-5(23)-6X, (B) H-ZSM-5(80), (B 1) H-ZSM-5(80)-3X and (B 2) H-ZSM-5(80)-6X catalysts

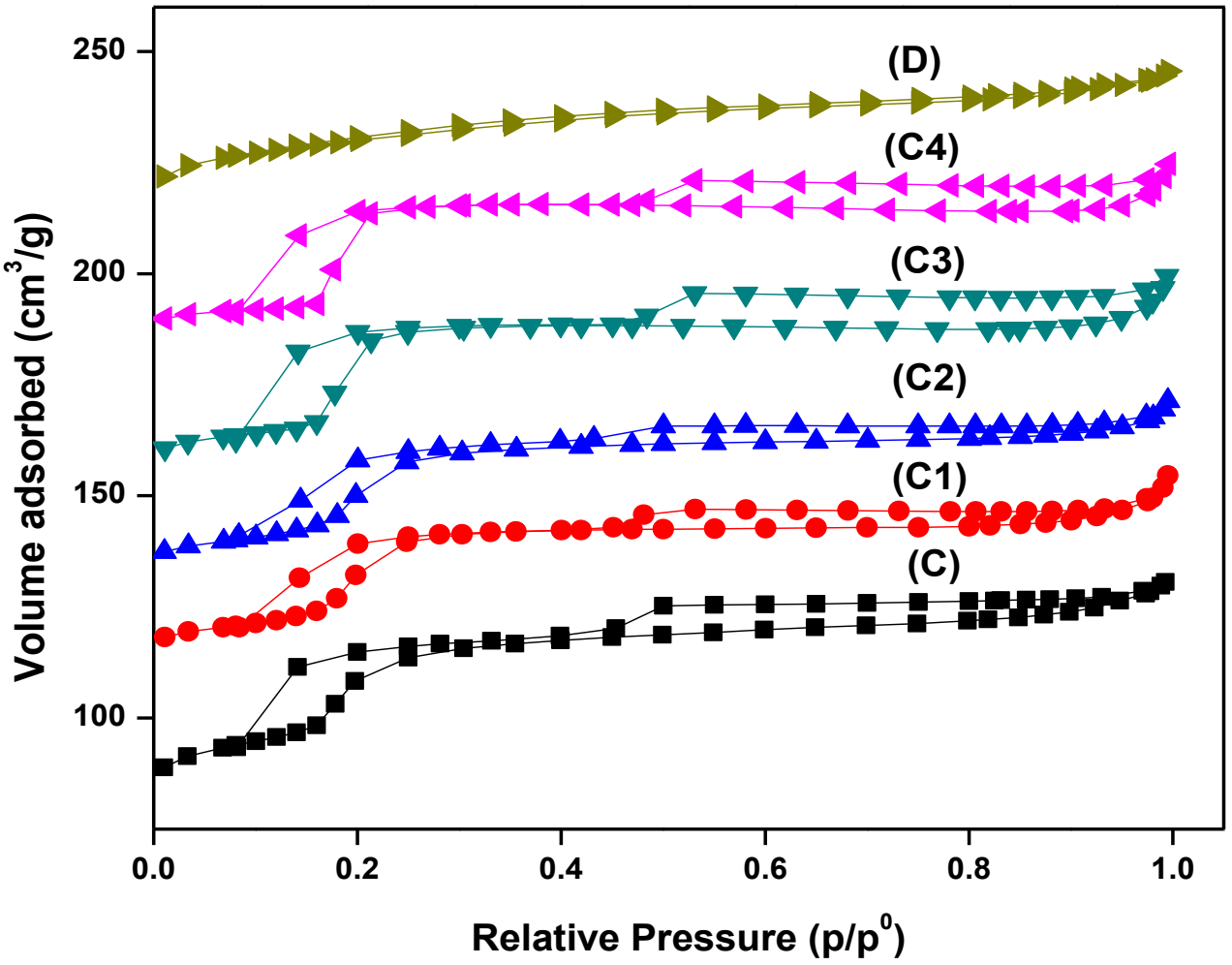

Figure 20 Nitrogen adsorption-desorption isotherms of of (C) H-ZSM-5(280), (C 1) H-ZSM-5(280)-3X, (C 2) H-ZSM-5(280)-6X, (C 3) H-ZSM 5(280)@CoreShell-1X, (C 4) H-ZSM-5(280)@CoreShell-2X and (D) H-ZSM-5(1500) catalysts

Table 8 Physicochemical properties of parent and modified ZSM-5 catalysts

Catalyst	BET (m^2/g)	V_{mic} (cm^3/g)	V_{tot} (cm^3/g)	Pore dia. (Å)
A	426	0.12	0.29	32.4
A1	411	0.11	0.28	33.4
A2	393	0.10	0.29	33.3
B	384	0.11	0.24	33.7
B1	357	0.10	0.22	36.0
B2	346	0.09	0.23	36.1
C	373	0.04	0.21	26.2
C1	356	0.03	0.22	26.5
C2	341	0.03	0.19	26.9
C3	382	0.02	0.21	24.6
C4	372	0.02	0.19	23.6
D	335	0.14	0.19	35.1

V_{mic} = micropore volume; V_{tot} = total pore volume.

(A) H-ZSM-5(23), (A 1) H-ZSM-5(23)-3X, (A 2) H-ZSM-5(23)-6X, (B) H-ZSM-5(80), (B 1) H-ZSM-5(80)-3X, (B 2) H-ZSM-5(80)-6X, (C) H-ZSM-5(280), (C 1) H-ZSM-5(280)-3X, (C 2) H-ZSM-5(280)-6X, (C 3) H-ZSM 5(280)@CoreShell-1X, (C 4) H-ZSM-5(280)@CoreShell-2X and (D) H-ZSM-5(1500) catalysts

4.1.3 Scanning Electron Microscopy:

SEM images of catalysts H-ZSM-5(23) (A), H-ZSM-5(80) (B), H-ZSM-5(280) (C), H-ZSM-5(280)-6X (C2), H-ZSM-5(280)@CoreShell-1X (C3) and H-ZSM-5(280)@CoreShell-2X (C4) are shown in Figure 21. The particles size was increased with increasing the Si/Al ratio. The image for H-ZSM-5 showed relatively large quadrangular prism-like crystallites. After silica deposition by the CLD method, the catalyst H-ZSM-5(280)-6X (C2) does not show any change in crystal size. However, catalyst H-ZSM-5(280)@CoreShell-1X (C3) and H-ZSM-5(280)@CoreShell-2X (C4) synthesized by core-shell method showed an increase in the crystal size as compared with catalyst H-ZSM-5(280) (C). The crystal size of H-ZSM-5(280)@CoreShell-1X (C3) and H-ZSM-5(280)@CoreShell-2X (C4) was increased at least 3 times as compared to the parent material. The crystal size of catalyst H-ZSM-5(280)@CoreShell-2X (C4) was slightly increased as compared to catalyst H-ZSM-5(280)@CoreShell-1X (C3).

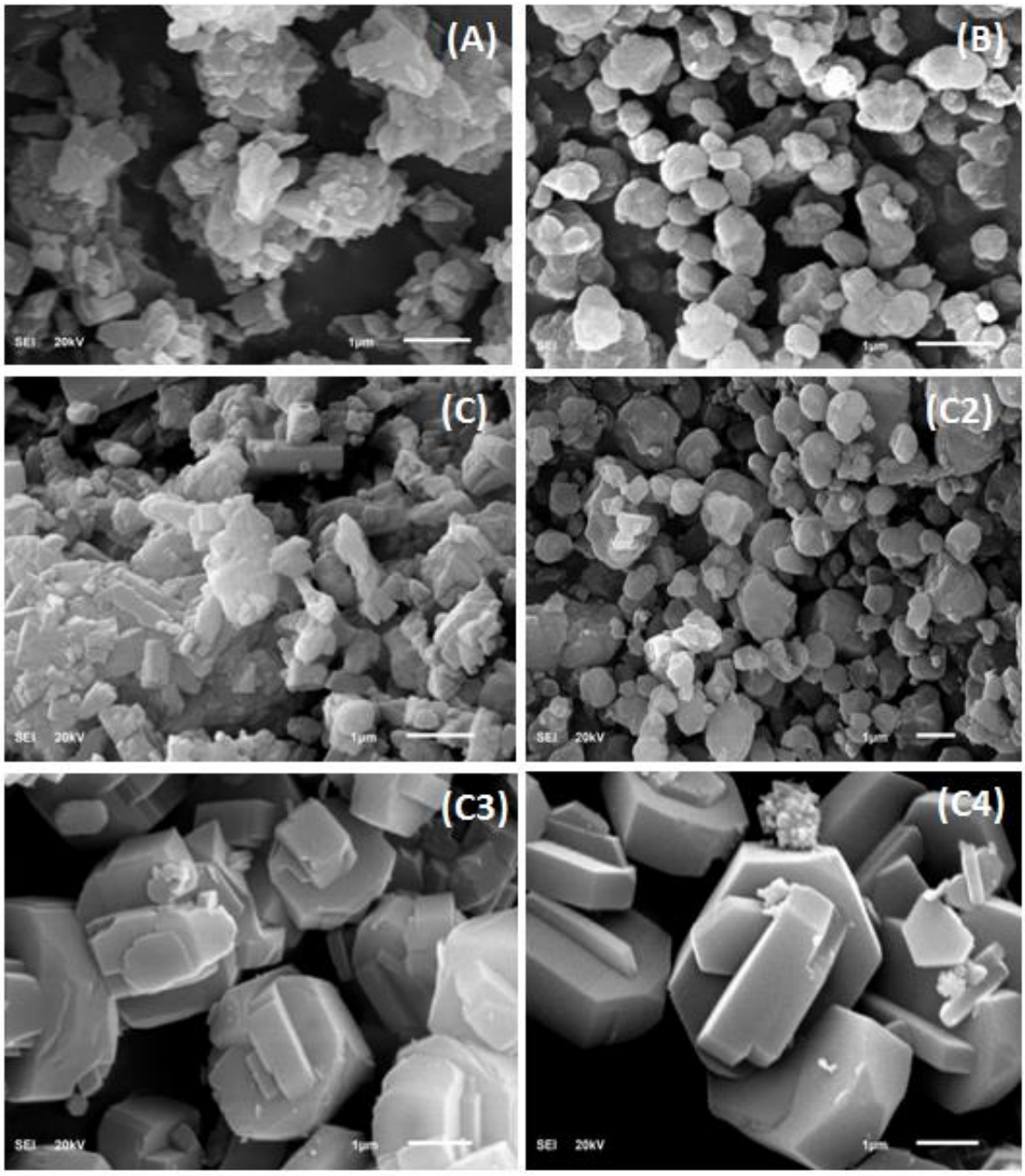

Figure 21 SEM images of H-ZSM-5(23) (A), H-ZSM-5(80) (B), H-ZSM-5(280) (C), H-ZSM-5(280)-6X (C2), H-ZSM-5(280)@CoreShell-1X (C3) and H-ZSM-5(280)@CoreShell-2X (C4) catalysts

4.1.4 Fourier Transform Infrared Spectroscopy (FT-IR)

Figure 21 shows the FT-IR spectra in the OH stretching region for catalyst H-ZSM-5(280) (C), H-ZSM-5(280)-6X (C2), H-ZSM-5(280)@CoreShell-2X (C4), and H-ZSM-5(1500) (D). All tested catalysts show a band at 3745 cm^{-1}, assigned to the terminal silanol groups. In the case of catalyst H-ZSM-5(280)-6X (C2), prepared using CLD method, the intensity of terminal silanol group was decreased as compared to the parent material [36]. A band at 3610 cm^{-1} is assigned to the presence of Brønsted acid sites and was observed for catalyst H-ZSM-5(280) (C). The peak intensity was lowered for catalyst H-ZSM-5(280)-6X (C2) and H-ZSM-5(280)@CoreShell-2X (C4) as compared to parent H-ZSM-5(280) (C). This clearly indicates that the concentration of Brønsted acid sites was reduced by the CLD and core-shell synthesis method.

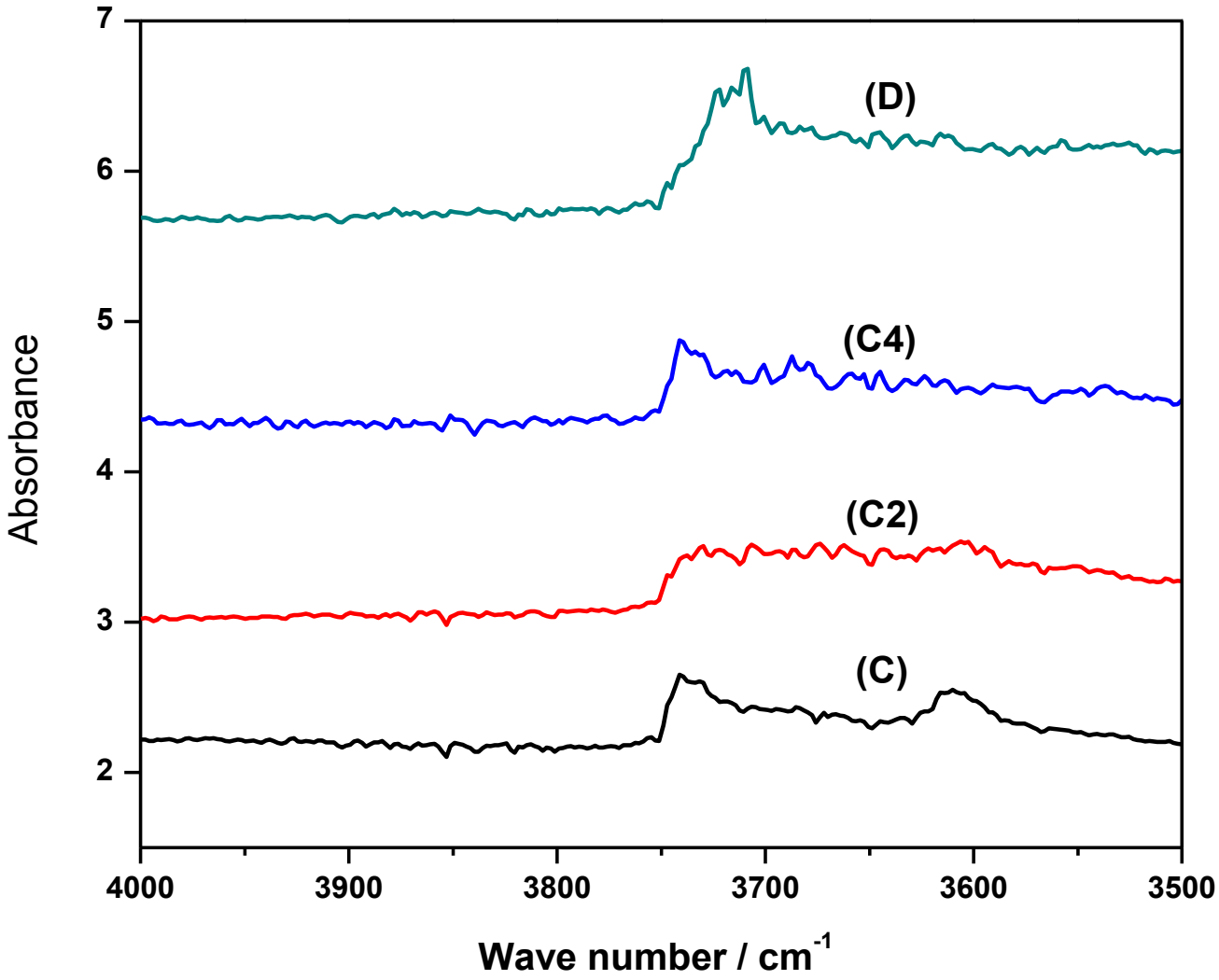

Figure 22 FT-IR spectra H-ZSM-5(280) (C), H-ZSM-5(280)-6X (C2), H-ZSM-5(280)@CoreShell-2X (C4), and H-ZSM-5(1500) (D) catalysts treated at 450°C for 1 hr under vacuum

The band 3745 cm^{-1} and 3610 cm^{-1} represents the OH- vibration of terminal silanol groups and Brønsted acid sites respectively.

4.1.5 Temperature-Programmed Desorption (TPD):

TPD profiles of desorbed ammonia are presented in Figure 23. Two peaks appeared for ZSM-5 zeolites. The peaks at a higher temperature correspond to the ammonia desorbed directly from the zeolites acid sites. The peaks appearing at a lower temperature were assigned to ammonia molecules adsorbed either on NH_4^+ species formed on Brønsted acid sites or on Na^+ cations [37]. From the areas of the peaks at a higher temperature, the number of acid sites was estimated and given in Table 9. As expected, the number of acid sites increased with a decrease in Si/Al ratio of H-ZSM-5 zeolites. No desorption peaks were observed for core-shell silicalite composite catalyst H-ZSM-5(280)@CoreShell-1X (C3) and H-ZSM-5(280)@CoreShell-2X (C4). In the case of catalyst prepared by CLD method, the increase in silica deposition cycles, decreased the total acidity of the resulting materials as shown in Table 9. The weakly adsorbing ammonia sites were 0.06 and 0.05 mmol g^{-1} for catalyst H-ZSM-5(280)-6X (C2) and H-ZSM-5(1500) (D), respectively.

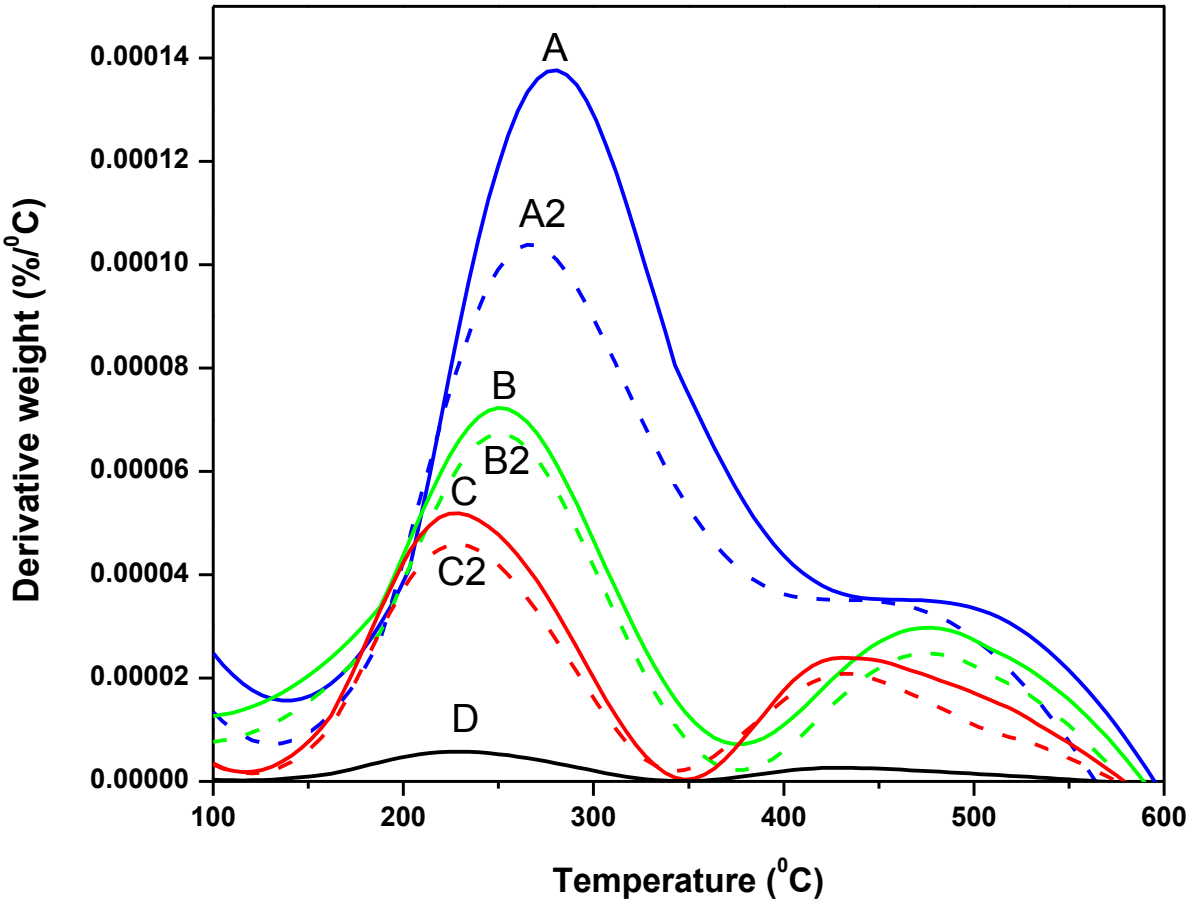

Figure 23 NH_3-TPD profiles of H-ZSM-5(23) (A), H-ZSM-5(23)-6X (A 2), H-ZSM-5(80) (B), H-ZSM-5(80)-6X (B 2), H-ZSM-5(280) (C), H-ZSM-5(280)-6X (C 2)and H-ZSM-5(1500) (D) catalysts

No desorption peaks were observed for core-shell silicalite composite catalyst H-ZSM-5(280)@CoreShell-1X (C3) and H-ZSM-5(280)@CoreShell-2X (C4).

Table 9 The number of acid sites using ammonia TPD

Catalyst	NH_3-TPD (mmol/g)		
	>300°C	300-550°C	TA
A	0.46	0.29	0.75
A1	0.31	0.16	0.47
A2	0.28	0.14	0.42
B	0.27	0.13	0.40
B1	0.21	0.11	0.33
B2	0.12	0.09	0.21
C	0.08	0.07	0.15
C1	0.07	0.05	0.12
C2	0.06	0.04	0.10
C3	nd	nd	nd
C4	nd	nd	nd
D	0.05	0.01	0.06

nd = not detectable; TA = total acidity.

(A) H-ZSM-5(23), (A 1) H-ZSM-5(23)-3X, (A 2) H-ZSM-5(23)-6X, (B) H-ZSM-5(80), (B 1) H-ZSM-5(80)-3X, (B 2) H-ZSM-5(80)-6X, (C) H-ZSM-5(280), (C 1) H-ZSM-5(280)-3X, (C 2) H-ZSM-5(280)-6X, (C 3) H-ZSM 5(280)@CoreShell-1X, (C 4) H-ZSM-5(280)@CoreShell-2X and (D) H-ZSM-5(1500) catalysts

4.1.6 External surface acidity Testing:

The external surface acidity of the zeolite was measured by cracking of 1,3,5 triisopropyl benzene (TIPB) using a fluidized-bed reactor at atmospheric pressure. The experiments were performed with 0.81 g of catalyst and 200 µl of TIPB at 550°C for 20s. The conversion of TIPB was found to be 51.37%, 14.09%, 0.71% for catalyst H-ZSM-5(280) (C), H-ZSM-5(280)-6X (C2) and H-ZSM-5(280)@CoreShell-2X (C4), respectively.

4.2 Catalyst Evaluation

In the catalytic reaction, more than 20 hydrocarbons were produced. These products were classified into eleven groups according to the expected reaction mechanism. These groups were; 1-butene (reactant), *cis*- and *trans*-2-butene, propylene (target product), ethylene, iso-butene, pentenes, hexenes, alkanes (C1-C6), aromatics (BTEX), and hydrocarbons with carbon number more than 8 (C8+, aromatics other than benzene, toluene, xylenes, and ethylbenzene, alkanes and alkenes; oligomerization and hydrogen transfer products). Table 10 summarizes the dependence of the detailed product distribution on the catalyst formulation, and the yield of propylene and ethylene at 550°C with modified ZSM-5 catalysts are presented in Figure 24.

The summarized products are plotted against the reaction temperature in Figures 25-27 for catalysts H-ZSM-5(280) (C), H-ZSM-5(280)-6X (C2) and H-ZSM-5(280)@CoreShell-2X (C4), respectively.

Table 10 Products distribution (C-wt %) in cracking of 1-butene using different catalysts at 1 bar, 550 ^{0}C (TOS =1 hr, GHSV =900 h^{-1})

	A	A1	A2	B	B1	B2	C	C1	C2	C3	C4	D
Total Acidity (mmol/g)	0.75	0.47	0.42	0.40	0.33	0.21	0.15	0.12	0.10	nd	nd	0.06
1-$C_4^=$ Conversion	100.00	100.00	98.34	100.00	100.00	97.90	98.30	97.84	97.81	96.92	95.29	91.57
Product distribution (C-wt %)												
1-butene	0.00	0.00	1.66	0.00	0.00	2.10	1.70	2.16	2.19	3.08	4.71	8.43
2-butene	0.00	1.06	3.48	0.00	1.02	4.35	3.54	5.50	5.53	6.36	9.73	16.49
Isobutylene	0.00	2.27	4.03	1.56	2.05	5.13	3.85	5.72	5.94	7.06	11.13	19.77
$C_2^=$	1.70	12.52	15.93	12.66	12.29	17.18	18.58	18.27	20.07	18.89	13.82	8.84
$C_3^=$	0.50	13.30	20.58	11.49	13.11	24.65	21.88	28.14	26.37	32.87	41.44	31.62
$C_5^=$	0.00	0.00	0.82	0.00	0.00	1.05	0.82	1.31	1.08	3.23	5.45	6.88
$C_6^=$	0.00	11.52	5.14	8.92	8.61	4.72	4.61	3.96	4.09	2.46	0.98	0.00
Alkanes (C_1-C_6)	14.80	32.91	27.12	35.60	32.60	22.89	22.11	17.23	17.86	14.39	7.08	4.59
Aromatics (BTEX)	50.50	18.75	12.96	19.67	19.71	11.35	12.46	11.15	10.23	6.33	0.00	0.00
C_8+	32.60	7.68	8.29	10.10	10.60	6.58	10.44	6.56	6.64	5.33	5.68	3.38
$C_2^= + C_3^=$	2.20	25.82	36.51	24.15	25.41	41.83	40.46	46.40	46.44	51.76	55.26	40.46
P/E ratio	0.29	1.06	1.29	0.91	1.07	1.43	1.18	1.54	1.31	1.74	3.00	3.58

(A) H-ZSM-5(23), (A 1) H-ZSM-5(23)-3X, (A 2) H-ZSM-5(23)-6X, (B) H-ZSM-5(80), (B 1) H-ZSM-5(80)-3X, (B 2) H-ZSM-5(80)-6X, (C) H-ZSM-5(280), (C 1) H-ZSM-5(280)-3X, (C 2) H-ZSM-5(280)-6X, (C 3) H-ZSM 5(280)@CoreShell-1X, (C 4) H-ZSM-5(280)@CoreShell-2X and (D) H-ZSM-5(1500) catalysts

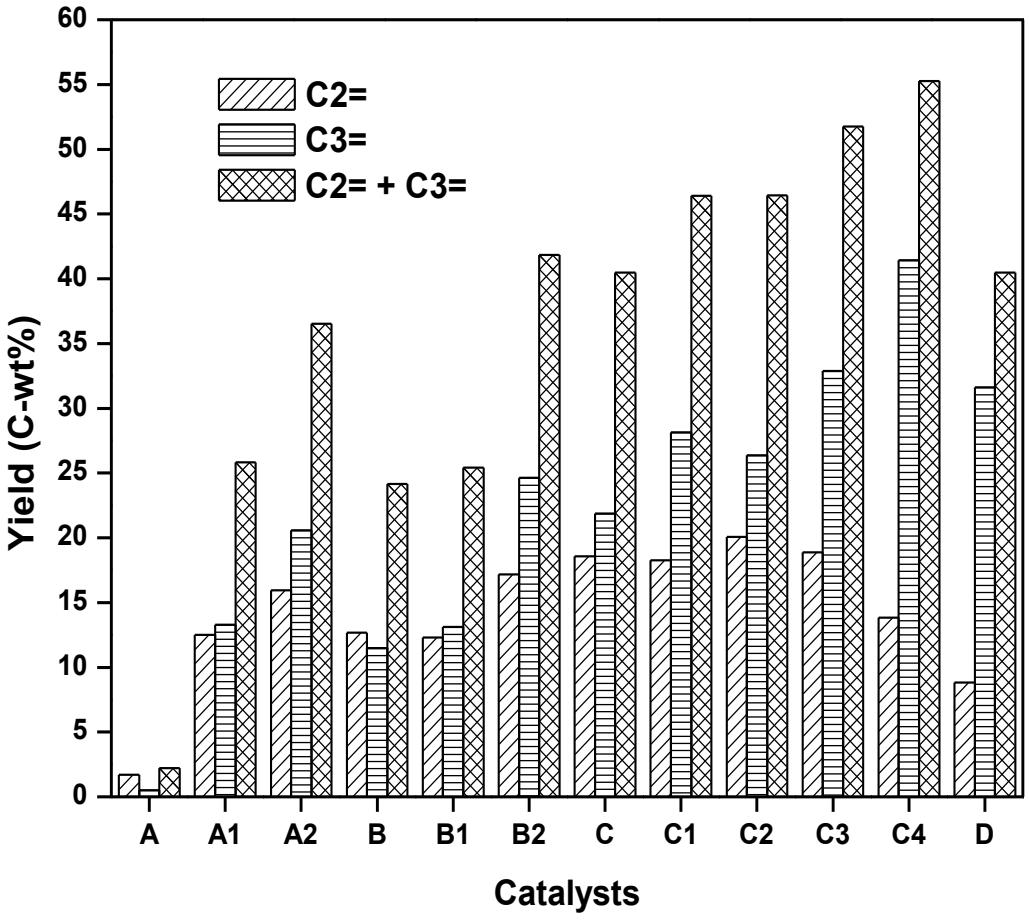

Figure 24 The yield of ethylene and propylene on catalytic cracking of 1-butene using A, A1, A2, B, B1, B2, C, C1, C2, C3, C4 and D catalysts

(A) H-ZSM-5(23), (A 1) H-ZSM-5(23)-3X, (A 2) H-ZSM-5(23)-6X, (B) H-ZSM-5(80), (B 1) H-ZSM-5(80)-3X, (B 2) H-ZSM-5(80)-6X, (C) H-ZSM-5(280), (C 1) H-ZSM-5(280)-3X, (C 2) H-ZSM-5(280)-6X, (C 3) H-ZSM 5(280)@CoreShell-1X, (C 4) H-ZSM-5(280)@CoreShell-2X and (D) H-ZSM-5(1500) catalysts

Catalyst H-ZSM-5(23) (A), which has both strong and weak acid sites showed higher amount of aromatics and C8+ as main products. The aromatics yield was lowered, when the Si/Al molar ratio of catalyst was increased from 23 to 1500 (Catalyst H-ZSM-5(23) (A) to H-ZSM-5(1500) (D)). This clearly shows that the formation of aromatics by hydrogen transfer reactions required strong acid sites. Upon continuous silica deposition by CLD method over catalyst H-ZSM-5(23) (A), the amount of aromatics was decreased due to the reduction of strong acid sites as evident from acidity measurements. The suppression of hydrogen transfer increased the amount of ethylene and propylene for catalyst H-ZSM-5(23)-6X (A2) as compared to catalyst H-ZSM-5(23)-3X (A1) and H-ZSM-5(23) (A). Similar observation was made for silica deposited catalysts H-ZSM-5(80)-3X (B1), H-ZSM-5(80)-6X (B2), H-ZSM-5(280)-3X (C1) and H-ZSM-5(280)-6X (C2). It has been reported [30][38] that the transformation of 1-butene involves two successive steps to produce propylene, i.e., dimerization of butenes and cracking of octene isomers. The $C_4^=$ molecules adsorb on acid sites of the catalysts to form a $[C_4]^+$ carbenium ion, which can react with another $C_4^=$ molecule to form the $[C_8]^+$ carbenium intermediate. This unstable intermediate is cracked to form propylene molecule and a $[C_5]^+$ carbenium ion via ß-scission mechanism [39][40]. The $[C_5]^+$ carbenium ion can further crack to propylene and ethylene or can desorb as C_5 hydrocarbons. The $[C_8]^+$ carbenium intermediate can also produce aromatics by dehydro-cyclization. Apart from this, the $[C_8]^+$ carbenium ion can further oligomerize with a $C_4^=$ molecule to form $[C_{12}]^+$ carbenium ion. The $[C_{12}]^+$ carbenium ion can then be converted to low molecular hydrocarbons by cracking/aromatization reactions. The commercially available ZSM-5 catalyst with SiO_2/Al_2O_3 ratio of 1500 (Catalyst D) showed the yield of propylene and ethylene about 31.62% and 8.84% at 550°C, respectively. However, the formation of isobutene (skeletal isomerization) was more for catalyst H-ZSM-5(1500) (D) as

compared to other catalysts (19.77%). The highest P/E ratio of 3.58 was observed for catalyst H-ZSM-5(1500) (D).

The summarized products are plotted against the reaction temperature in Figures 25-27 for catalysts H-ZSM-5(280) (C), H-ZSM-5(280)-6X (C2) and H-ZSM-5(280)@Core-Shell-2X (C4), respectively.

Over catalyst H-ZSM-5(280) (C) (Figure 25), double bond isomerization was the main reaction occurring in the temperature range 150-200°C. At 250°C, the main products were alkenes (including propylene) and C8+. Increasing the reaction temperature to 350°C, the formation of alkenes was reduced dramatically, and the formation of alkanes and aromatics became dominant. However, as the temperature was further increased, the formations of alkenes, including propylene, gradually increased in the temperature range 350-550°C. The percentage of propylene and ethylene over catalyst H-ZSM-5(280) (C) increased with the reaction temperature up to 550 °C to reach 21.88% and 18.58% at 550°C, respectively.

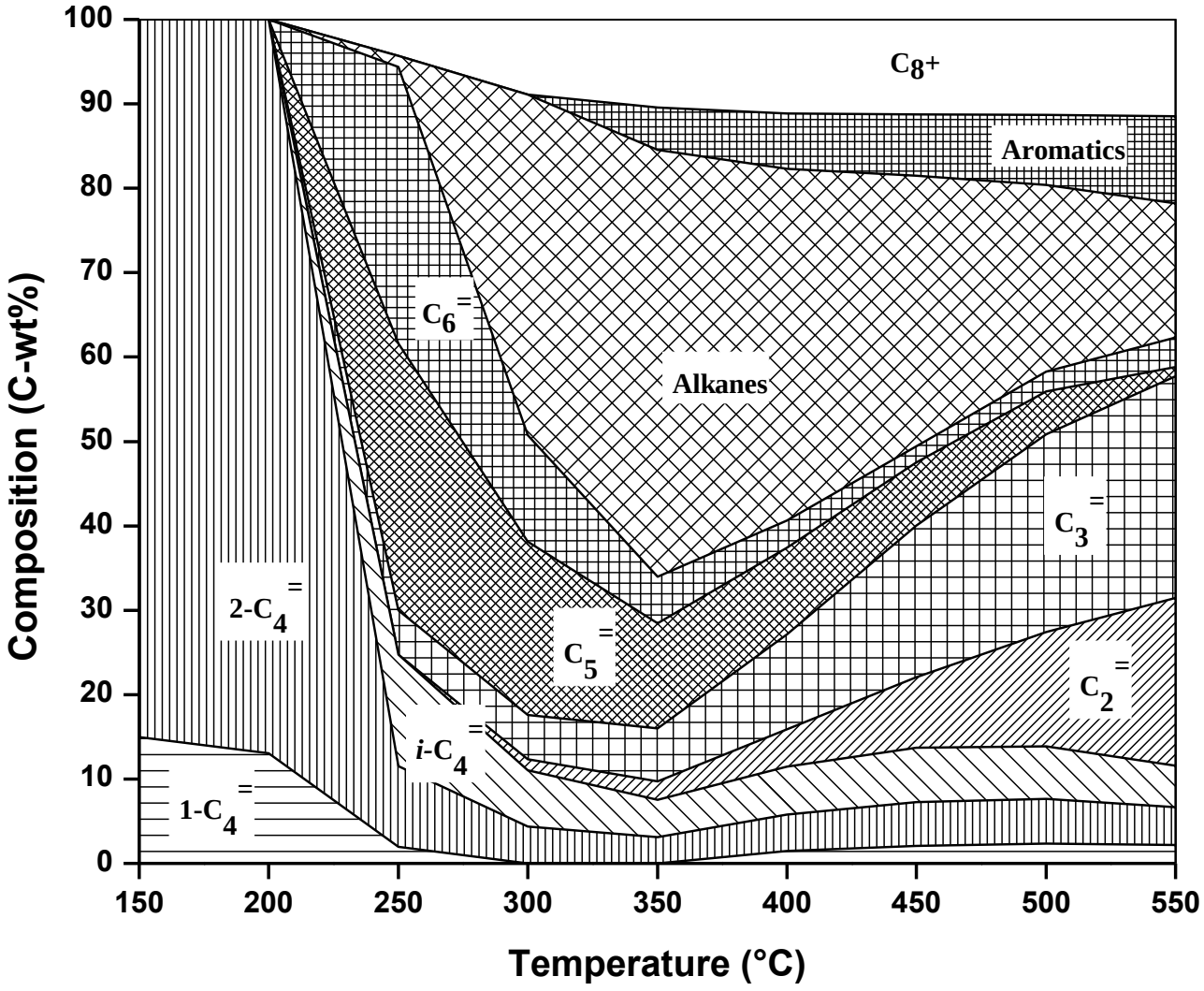

Figure 25 Products distribution (C-wt %) in catalytic cracking of 1-butene using Catalyst C [ZSM-5(280)] as catalysts at 1 bar, TOS =1 hr, GHSV =900 h^{-1}

The yield of propylene and ethylene over catalyst H-ZSM-5(280)-6X (C2) increased with the reaction temperature and to reach 26.37% and 20.07% at 550°C, respectively (Figure 26). The catalyst H-ZSM-5(280)-3X (C1) and H-ZSM-5(280)-6X (C2) showed almost similar activity. This showed that triplicate deposition of silica on catalyst H-ZSM-5(280) (C) is sufficient and further deposition does not enhance much the catalyst activity.

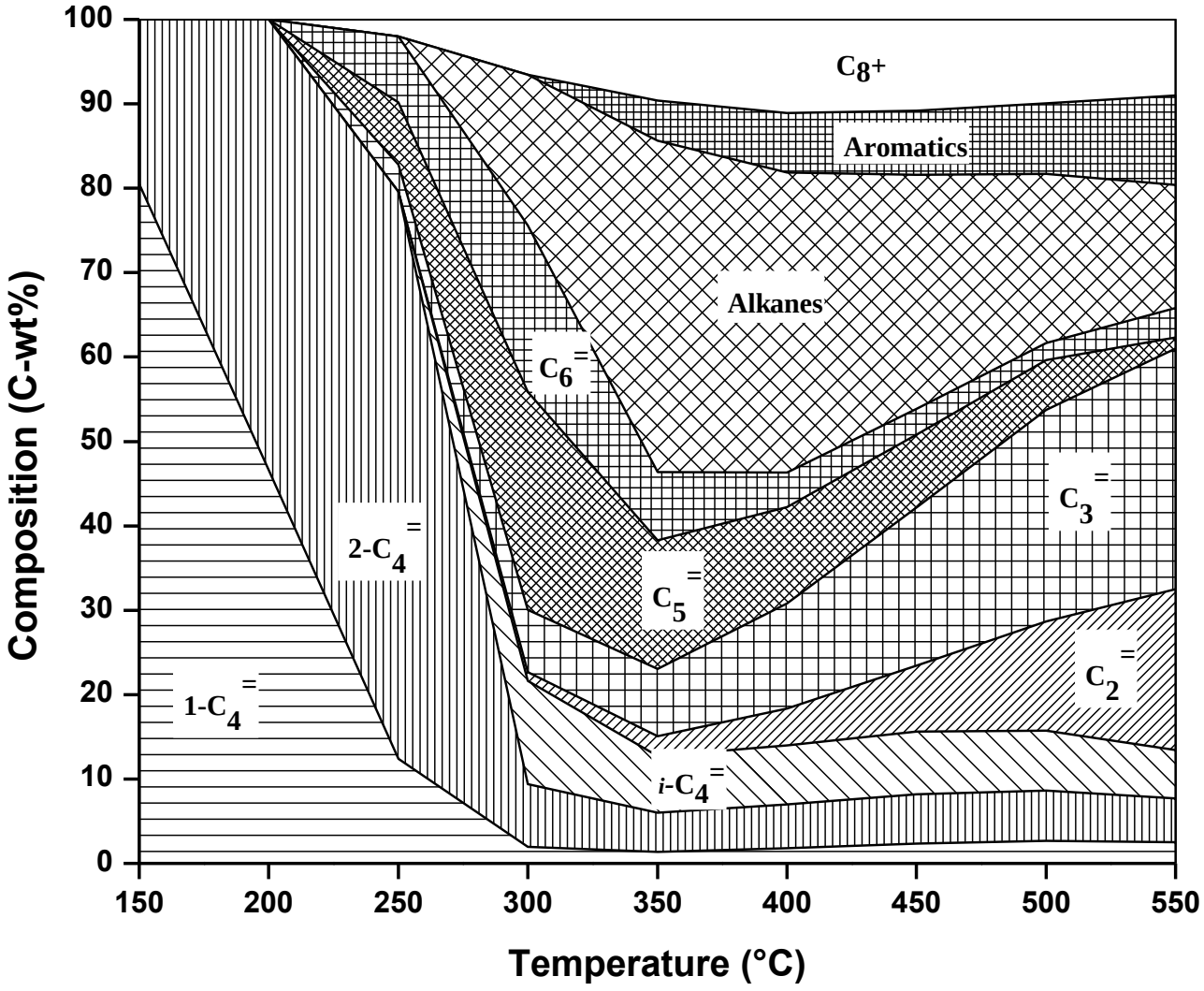

Figure 26 Products distribution (C-wt %) in catalytic cracking of 1-butene using catalyst C2 [ZSM-5(280)-6X] at 1 bar, TOS =1 hr, GHSV =900 h^{-1}

Core-shell silicalite composite catalyst H-ZSM-5(280)@Core-Shell-2X (C4) (Figure 27) showed double bond isomerization was the main reaction occurring in the temperature range 150-200°C. At 250°C, the main products were 1-butene and 2-butene isomers with very small percentages of other alkenes. As the temperature increased to 300°C, the formation of alkenes became predominant, and the formations of alkanes and C8+ were limited to small percentages. Further increase in reaction temperature to 550°C, the yield of propylene and ethylene reached a maximum of 41.44% and 13.82%, respectively. Aromatics were not formed over H-ZSM-5(280)@Core-Shell-2X (C4) catalyst in the temperature range from 150-550°C, as this requires strong acid sites for hydrogen transfer reactions. The higher propylene yield is related to the presence silanol groups which act as very weak acid sites at higher temperatures. Apart from weak acid sites, the presence external surface acidity of catalyst H-ZSM-5(280)@Core-Shell-2X (C4) was much lower as compared to catalyst H-ZSM-5(280) (C) and H-ZSM-5(280)-6X (C2) as evident from TIPB cracking reaction. The formation of ethylene was lowered for catalyst H-ZSM-5(280)@Core-Shell-2X (C4) as compared to catalyst H-ZSM-5(280) (C), H-ZSM-5(280)-3X (C1), H-ZSM-5(280)-6X (C2) and H-ZSM-5(280)@Core-Shell-1X (C3). The presence of more isomerized product in catalyst H-ZSM-5(280)@Core-Shell-2X (C4) showed that direct cracking of 1-butene to ethylene was lowered. Similar observation was made for catalyst H-ZSM-5(280)@Core-Shell-2X (C4) and catalyst H-ZSM-5(1500) (D), as catalyst H-ZSM-5(1500) (D) showed only 8.84% of ethylene yield with higher isomerized product yield 36.26%.

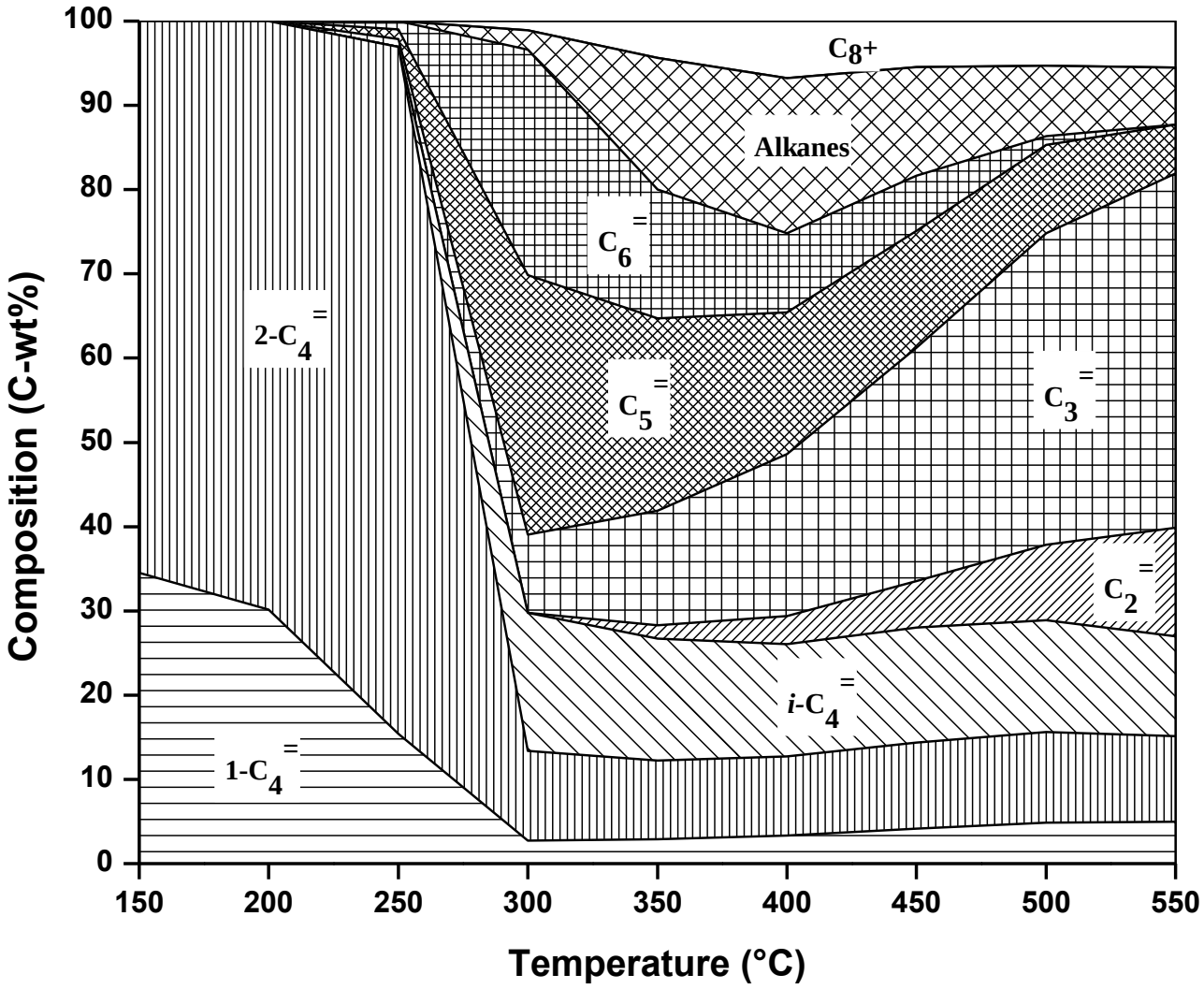

Figure 27 Products distribution (C-wt %) in catalytic cracking of 1-butene using catalyst C4 [ZSM-5(280)-core-shell 2X] at 1 bar, TOS =1 hr, GHSV =900 h^{-1}

4.3 Other Side Reactions

The formation of alkanes, aromatics, and isomerization products for catalyst H-ZSM-5(280) (C), H-ZSM-5(280)-3X (C1), H-ZSM-5(280)-6X (C2), H-ZSM-5(280)@Core-Shell-1X (C3), H-ZSM-5(280)@Core-Shell-2X (C4) and H-ZSM-5(1500) (D) was shown in Figure 28. In our previous study [26], we found that by increasing the Si/Al molar ratio from 23 to 280 the formation of aromatic and alkanes was decreased and the yield of isomerization products was increased. We observe the similar trend for catalyst catalyst H-ZSM-5(280) (C), H-ZSM-5(280)-3X (C1), H-ZSM-5(280)-6X (C2), H-ZSM-5(280)@Core-Shell-1X (C3), H-ZSM-5(280)@Core-Shell-2X (C4) and H-ZSM-5(1500) (D). In the case of catalysts H-ZSM-5(280)-3X (C1) to H-ZSM-5(280)@Core-Shell-2X (C4), the formation of alkanes and aromatic was lowered as compared to parent material (H-ZSM-5(280) (C)). This shows that surface modification by both CLD and core-shell silicalite composite method decreases the acidity, which reduces the formation of alkanes and aromatics through hydrogen transfer reactions. The formation of isomerization products both double bond isomerization and skeletal isomerization was increased from catalyst catalyst H-ZSM-5(280) (C), H-ZSM-5(280)-3X (C1), H-ZSM-5(280)-6X (C2), H-ZSM-5(280)@Core-Shell-1X (C3), H-ZSM-5(280)@Core-Shell-2X (C4) and H-ZSM-5(1500) (D).

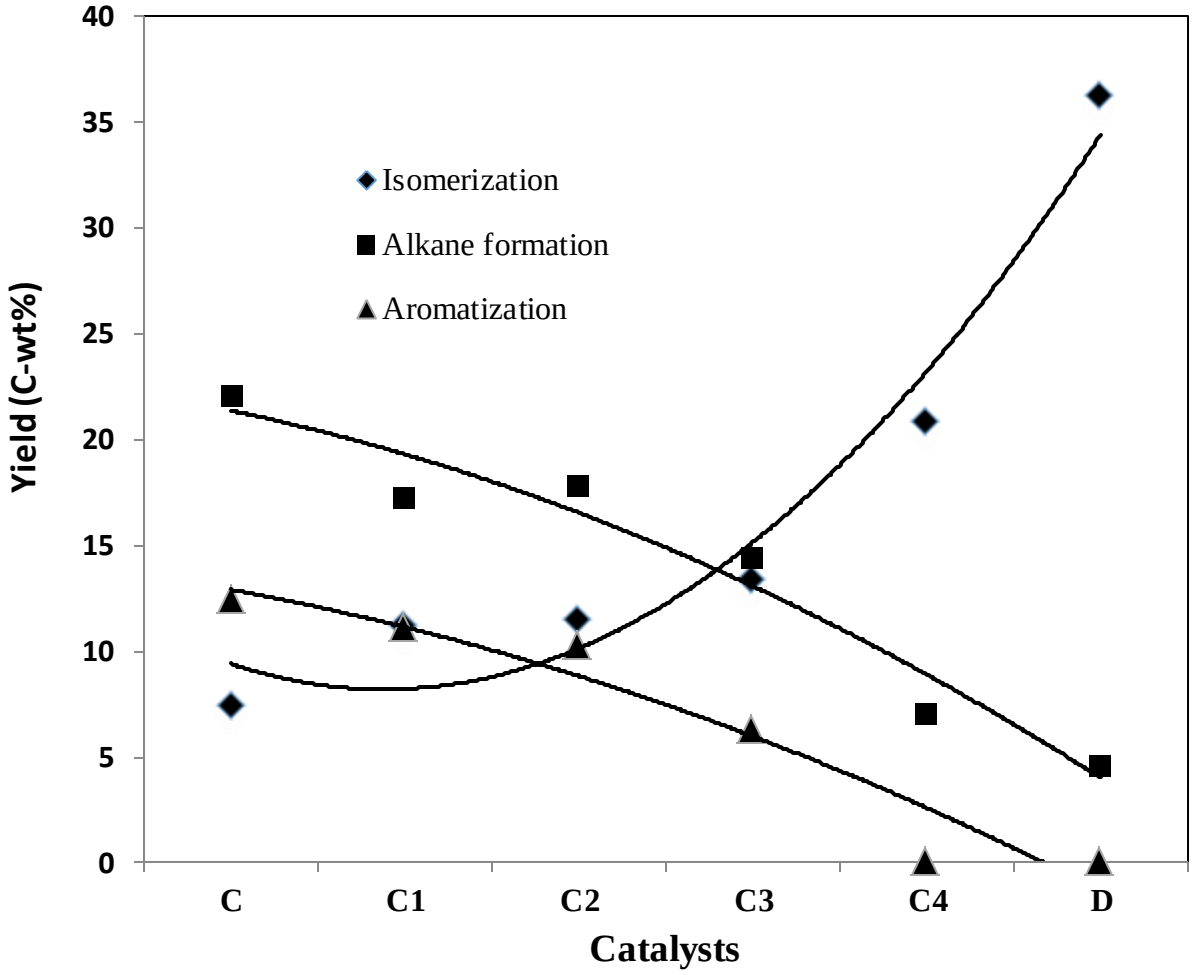

Figure 28 The yield of aromatics, alkanes and isomerization products on catalytic cracking of 1-butene using C, C1, C2, C3, C4 and D catalysts

(C) H-ZSM-5(280), (C 1) H-ZSM-5(280)-3X, (C 2) H-ZSM-5(280)-6X, (C 3) H-ZSM 5(280)@CoreShell-1X, (C 4) H-ZSM-5(280)@CoreShell-2X and (D) H-ZSM-5(1500) catalysts

4.4 Time on stream study

Catalyst stability was plotted for catalysts H-ZSM-5(280)@Core-Shell-2X (C4) and H-ZSM-5(1500) (D). Catalyst H-ZSM-5(1500) (D) was chosen to compare with catalyst H-ZSM-5(280)@Core-Shell-2X (C4) due to the high P/E ratio it afforded. The results, presented in Figure 29, show that catalyst H-ZSM-5(280)@Core-Shell-2X (C4) was stable for 50 hours under the 1-butene stream, whereas catalyst H-ZSM-5(1500) (D) deactivated faster. The yields of propylene and ethylene remained the same for 50 hours over catalyst H-ZSM-5(280)@Core-Shell-2X (C4).

The formation of isobutene increased from 19% (TOS = 1h) to 34% (TOS = 50h) for catalyst H-ZSM-5(1500) (D) resulting the catalyst deactivation. The coke formation of catalyst H-ZSM-5(280)@Core-Shell-2X (C4) and H-ZSM-5(1500) (D) was found to be 0.73% and 1.5%, respectively. These results indicate excellent catalyst stability of core-shell silicate composite as compared to catalyst H-ZSM-5(1500) (D).

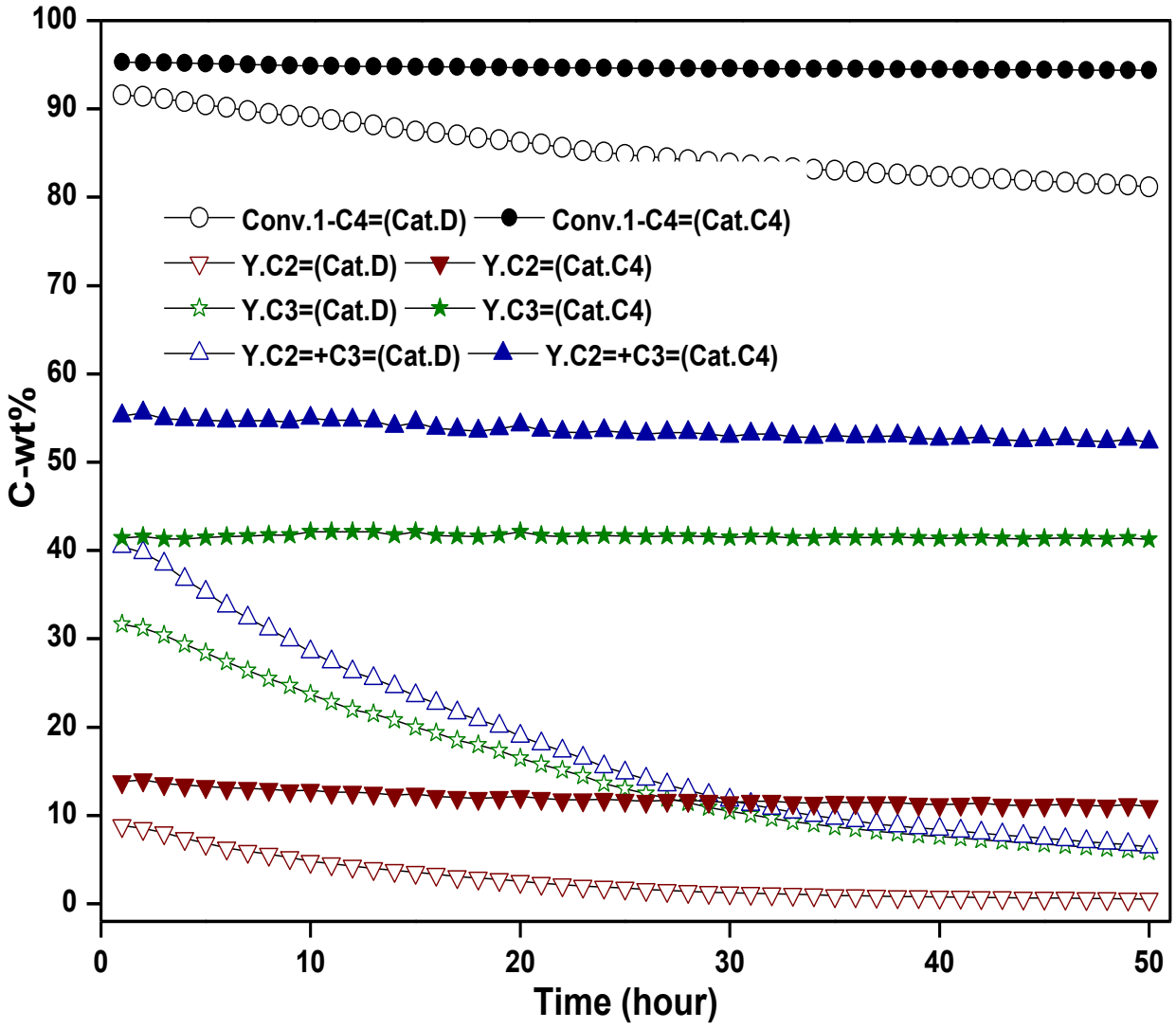

Figure 29 Time on stream study using catalysts H-ZSM-5(280)@Core-Shell-2X (C4) and H-ZSM-5(1500) (D) over the 1-butene stream for 50 hours

CHAPTER 5

KINETIC MODELING

In this part of the study, kinetic modeling was conducted to evaluate the activation energies of 1-butene cracking over H-ZSM-5(1500) (D), It has been reported [30][38] that the transformation of 1-butene involves two successive steps to produce propylene, i.e., dimerization of butenes and cracking of octene isomers. The $C_4^=$ molecules adsorb on acid sites of the catalysts to form a $[C_4]^+$ carbenium ion, which can react with another $C_4^=$ molecule to form the $[C_8]^+$ carbenium intermediate. This unstable intermediate is cracked to form propylene molecule and a $[C_5]^+$ carbenium ion via ß-scission mechanism [39][40]. Apart from this, the $[C_8]^+$ carbenium ion can further oligomerize with a $C_4^=$ molecule to form $[C_{12}]^+$ carbenium ion. The $[C_{12}]^+$ carbenium ion can then be converted to low molecular hydrocarbons like $[C_6]^+$ carbenium ion via ß-scission mechanism.

5.1 Model Assumptions

There are several reaction possibilities along with various suggested mechanisms and different steps involved. In order to simplify the model and ease the model development so reasonable parameter estimation can be achieved; the following is assumed:

- Mass transfer limitation is negligible
- Negligible catalyst deactivation
- Effectiveness factor is unity

Model assumes only catalytic conversion

5.2 Model Development

Strategy of lumping the alkene components that have the same number of carbons in their structure is effective strategy for simplifying the kinetic modeling and the involved rate equations, so the following reaction mechanism has been proposed:

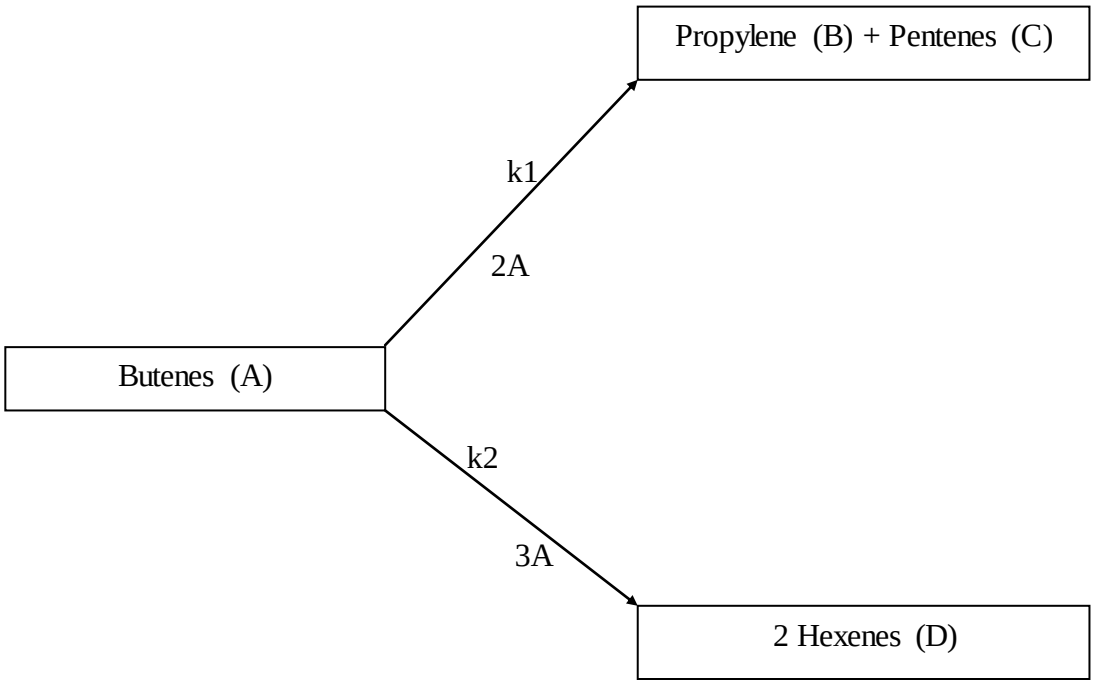

The notation used in the scheme will be used along this report, the notation includes:

A ≡ Butenes,

B ≡ Propylene,

C ≡ Pentene,

and D ≡ Hexene.

The reaction mechanism:

$$2A \rightarrow B + C$$

$$3A \rightarrow 2D$$

Then the rate equations for the above reactions:

$$r_1' = k_1 C_A^2$$

$$r_2' = k_2 C_A^3$$

The rate equations for the different lumps can be deduced from the reaction network and with the help of suggested assumptions. So the rate equations for each lump can be written as:

Disappearance of Butenes:

$r_A = \frac{dC_A}{d\tau'} = -r_1' - r_2' = -k_1 C_A^2 - k_2 C_A^3$

Formation of Propylene:

$r_B = \frac{dC_B}{d\tau'} = 0.5\ r_1' = 0.5\ k_1 C_A^2$

Formation of Pentenes:

$r_C = \frac{dC_C}{d\tau'} = 0.5\ r_1' = 0.5\ k_1 C_A^2$

Formation of Hexenes:

$r_D = \frac{dC_D}{d\tau'} = \frac{2}{3} r_2' = \frac{2}{3} k_2 C_A^3$

The concentration can be written as:

$$C_i = \frac{y_i \, F_{TM}}{MW_i \vartheta}$$

Hence the equations can be reformulated in terms of fractions as:

Disappearance of Butenes:

$r_A = \frac{dY_A}{d\tau'} = -r_1' - r_2' = -k_1 \, Y_A^2 - k_2 Y_A^3$

Formation of Propylene:

$r_B = \frac{dY_B}{d\tau'} = 0.5 \; r_1' = 0.5 \, k_1 \, Y_A^2$

Formation of Pentenes:

$r_c = \frac{dY_C}{d\tau'} = 0.5 \; r_1' = 0.5 \, k_1 \, Y_A^2$

Formation of Hexenes:

$r_D = \frac{dY_D}{d\tau'} = \frac{2}{3} \, r_2' = \frac{2}{3} \, k_2 Y_A^3$

The rate constants k_i can also be written using Arrhenius formula as:

$$k_i = k_{i0} \; \exp\left(-\frac{E_i}{R} \left(\frac{1}{T} - \frac{1}{T_0} \right) \right)$$

Where:

k_{i0} : the pre-exponential factor,

E_i: the activation energy of the reaction i, and

and T_0: the centering temperature (average of all the temperatures).

5.3 Model Discrimination and Determination of Model Parameters

Non-linear regression method was applied in estimating the parameters of the kinetic model. For model evaluation, mole balance equations were combined with reaction rate constants (temperature dependent term) with the concentration of various species expressed in the form of mole fractions. These expressions were substituted in the ODE system of equations and then, this system was solved numerically together with a fitting of the least square for the analyzed data obtained experimentally. MATLAB ODE45 as subroutine (which uses Runge-Kutta-Gill method) was used for parameter estimation. For accurate estimation for the parameters of the model; the experimental runs were performed at seven different temperatures (250, 275, 300, 325, 350, 375 and 400^{o}C) and five different contact times of 1.0, 1.5, 2.0, 2.5 and 3.0 seconds.

In model evaluation the criteria that was followed considered that the parameters of kinetic model should comply with the principles of physics, the optimization objective function was to reduce the sum of the squares of the residuals between the experimental data and the predicted values by the model and the value of the determination coefficient (R^2) to be as close to one.

The estimated values of the parameters of the model together with their 95% confidence intervals are presented in Table 11. From the table it can be seen that the estimated apparent activation energies of the formation of firstly propylene and pentenes and secondly the formation of hexenes at the 250-400 ^{o}C temperature range are 7.6199 and 3.1265 kcal/mol respectively. This indicates that the H-ZSM-5(1500) (D) at the temperature range of 250-400^{o}C is more selective

towards the formation of hexenes, but as increasing the temperature over 400^{o}C these hexenes are expected to crack to give propylene as can be deduced from the results of catalyst H-ZSM-5(1500) (D) at 550^{o}C TOS =1 hr, GHSV =900 h^{-1} in table 10.

Table 11 Estimated values of kinetic parameters at 95% confidence intervals

Parameters	Values	Model discrimination	Values
k_1^{o} (m^3/mol.s)	0.1053 ± 0.0061	Correlation coefficient, R^2	0.9787
k_2^{o} (m^6/mol^2.s)	0.2372 ± 0.0148	Sum of squares, SS	0.0713
E_1 (kcal/mol)	7.6199 ± 0.2990		
E_2 (kcal/mol)	3.1265 ± 0.3765		

Butenes conversion was plotted versus contact time as shown in Figure 30 for both the experimental and model predicted values. It can be seen that the model agrees reasonably to the experimental data.

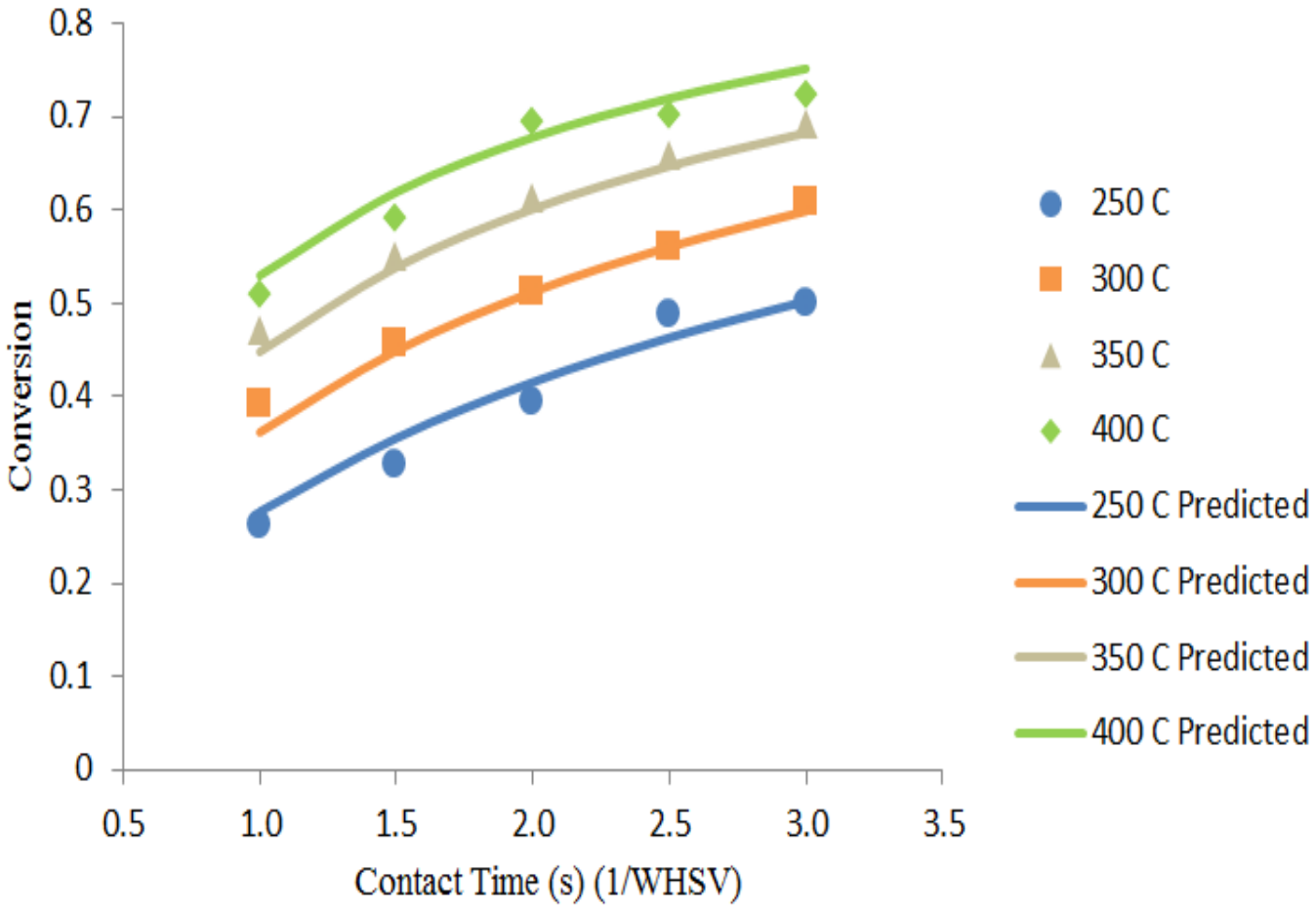

Figure 30 Conversion of 1-butene against contact time for both experimental and model predicted

Propylene yield was plotted versus contact time as shown in Figure 31 for both the experimental and model predicted values. It can be seen that the model agrees reasonably to the experimental data.

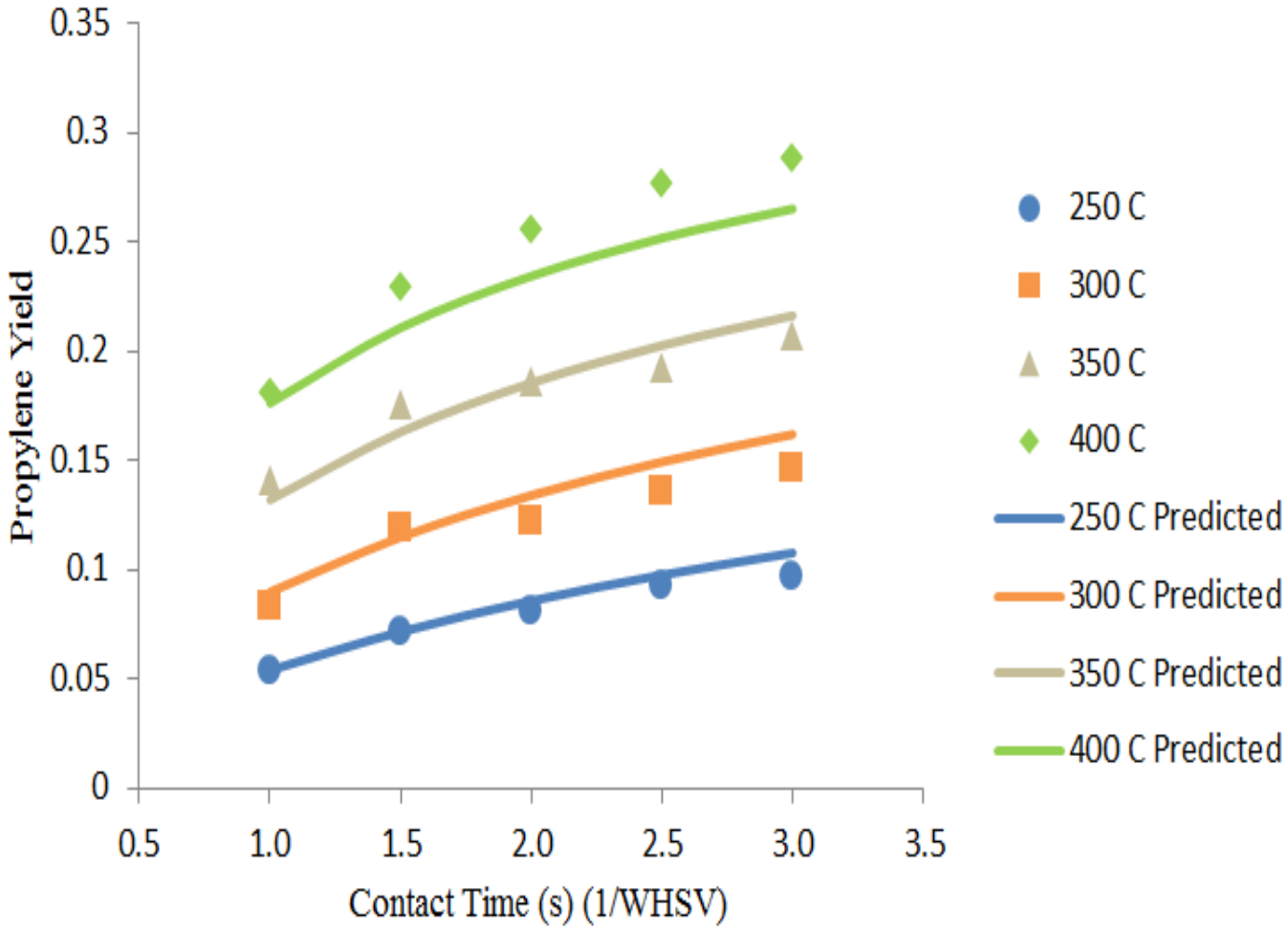

Figure 31 Experimental vs model predicted values for Propylene yield

To further show overall agreement between the experimental data and model predicted values, a parity plot as shown in Figure 32 was plotted. It can be concluded from the Figure that the model reasonably predicts the 1-butene cracking over H-ZSM-5(1500) (D) catalyst and also the model discrimination values of 0.9787 and 0.0713 for correlation coefficient (R^2) and sum of squares respectively.

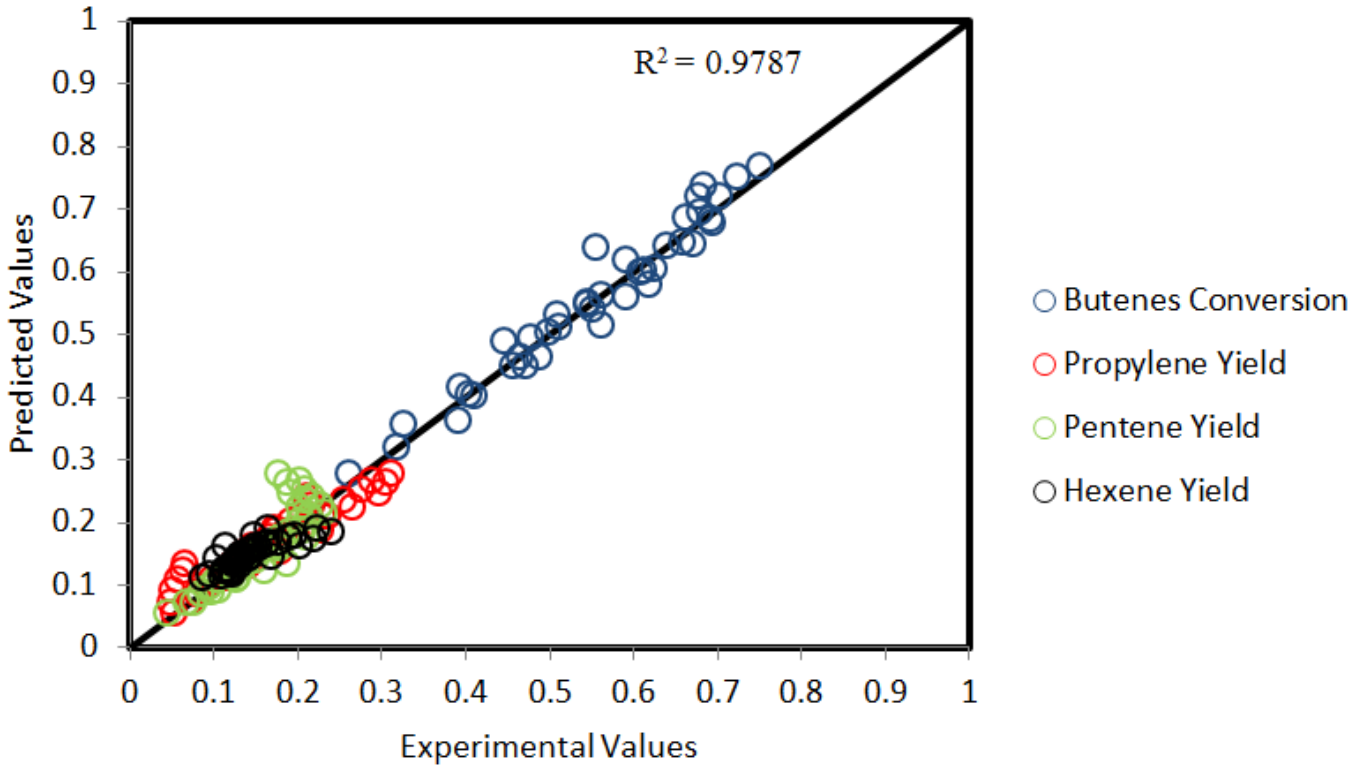

Figure 32 Parity plot between the experimental data and model predicted values

CHAPTER 6

CONCLUSIONS AND RECOMMENDATIONS

1.1 Conclusions

1-butene cracking is investigated to produce propylene as on-purpose propylene technology using ZSM-5 catalysts with different Si/Al and modifying the these catalysts by silica deposition using chemical liquid deposition (CLD) method as well as core-shell silicalite composite.

From the comparison of these catalysts 'with different Si/Al and with different degree of modification' the following can be concluded:

1. Core-shell composite showed higher propylene yield for catalytic cracking of 1-butene as compared to CLD method.
2. The higher propylene yield and stability is related to effective surface passivation as observed in external surface acidity measurements as well as FT-IR.
3. Maximum propylene and light olefins yields of 44.44 C-wt.% and 55.26 wt.%, respectively, were achieved over (C 4) H-ZSM-5(280)@CoreShell-2X.
4. Silica deposited using CLD method showed P/E ratio of 1.7, whereas core-shell silicalite composite has P/E ratio of 3.0.
5. The effective control of acid sites allows the reduction of hydrogen transfer reactions and hence, minimizing undesired products such as alkanes and aromatics.
6. It was found that aromatics formation decreased with the increase in light olefins formation.
7. The coke formation over core-shell silicalite composite was found to be 50% less than catalyst D, indicating better stability.

8. Results of the kinetic study showed that the estimated apparent activation energies on H-ZSM-5(1500) (D) for the formation of firstly propylene and pentenes and secondly the formation of hexenes at the 250-400^{o}C temperature range are 7.6199 and 3.1265 kcal/mol.

1.2 Recommendations

The following points are suggested for future work:

1. Optimize the core-shell silcalite treated catalysts so the best number of cycles to produce the highest propylene yields can be reached.
2. Kinetic modeling based on molecular description is desired. This will give better insight on the effect of the different Si/Al ratios and the total acidity on the reaction pathways for the production of propylene.

REFERENCES

[1] J.S. Plotkin, Catal. Today 106 (2005) pp. 10-14.

[2] Nexant, Propylene Technology: The Next Generation. (2009) pp. 2-4.

[3] A.M. Aitani, Propylene Production. In: Encyclopedia of Chemical Processing, Taylor and Francis: New York, (2007) pp. 2461-2466.

[4] S. Moolji, Petrochemical Scenario Across Continents: What is Happening in The World of Polypropylene?. IOCL Petrochemical ConClave, (2014).

[5] NexantThinking, On-Purpose Propylene in an Era of Uncertainty. (2015) pp. 1-14.

[6] Chemsystems, Evolving Propylene Sources-Solution to Shortages? (2012), pp. 2-6.

[7] X. Zhu, X. Li, S. Xie, S. Liu, G. Xu, W. Xin, S. Huang, L. Xu, Catal. Surv. from Asia 13 (2009) pp.1-8.

[8] Propylene via Metathesis. Intratec Solutions LLC, (2013) pp 11-12.

[9] R. Sleep, Propylene and Polypropylene (2012) pp. 1-12.

[10] J.S. Plotkin, Understanding The Global Petrochemical Industry: Propylene. IHS, (2015) pp. 2-4.

[11] H. Hattori, Y.Ono, Solid Acid Catalysis: From Fundamentals to Applications, Pan Stanford Publishing: Danvers MA , (2015) pp. 23–42.

[12] A. Bhan, Y. V Joshi, W.N. Delgass, K.T. Thomson, J. Phys. Chem. B 107 (2003) pp. 10476–10487.

[13] T. Blasco, Chem. Soc. Rev. 39 (2010) pp.4685–4702.

[14] A.G. Stepanov, M. V. Luzgin, V.N. Romannikov, K.I. Zamaraev, Catal. Letters 24 (1994)

pp. 271–284.

[15] Y. V. Kissin, Catal. Rev. 43 (2001) pp. 85–146.

[16] J. Abbot, A. Corma, B.W. Wojciechowski, J. Catal. 92 (1985) pp. 398–408.

[17] J. Li, H. Ma, H. Zhang, Q. Sun, W. Ying, A.C. Preparation, 9 (2015) pp. 11–15.

[18] L. Li, J. Gao, C. Xu, X. Meng, 116 (2006) pp. 155–161.

[19] L. Lin, C. Qiu, Z. Zhuo, D. Zhang, S. Zhao, H. Wu, Y. Liu, M. He, J. Catal. 309 (2014) pp. 136–145.

[20] P.K.D.H. of Z.S. and T. S. M. Auerbach, K. A. Carrado, Handbook of Zeolite Science and Technology, 2011.

[21] X. Zhu, S. Liu, Y. Song, L. Xu, Appl. Catal. A Gen. 288 (2005) pp 134–142.

[22] J. Lu, Z. Zhao, C. Xu, A. Duan, X. Wang, P. Zhang, J. Porous Mater. 15 (2008) pp. 213–220.

[23] E. Epelde, P. Vasco, E. Herriko, A.G. Gayubo, P. Vasco, E. Herriko, M. Olazar, P. Vasco, E. Herriko, E. Epelde, A.G. Gayubo, M. Olazar, J. Bilbao, A.T. Aguayo, (2015).

[24] J. Li, H. Ma, Q. Sun, W. Ying, D. Fang, Fuel Process. Technol. 134 (2015) pp. 32–38.

[25] P. Zeng, Y. Liang, S. Ji, B. Shen, H. Liu, B. Wang, H. Zhao, M. Li, J. Energy Chem. 23 (2014) pp. 193–200.

[26] A. Palani, T. I. Bhuiyan, M. N. Akhtar,A. M. Aitani, S. S. Al-Khattaf, H. Hattori, ACS Catal., 4 (2014) pp. 4205–4214.

[27] S. Zheng, H.R. Heydenrych, H.P. Röger, A. Jentys, J.A. Lercher, Top. Catal. 22 (2003) pp. 101–106.

[28] D. Van Vu, M. Miyamoto, N. Nishiyama, Y. Egashira, K. Ueyama, J. Catal. 243 (2006) pp. 389–394.

[29] D. Van Vu, M. Miyamoto, N. Nishiyama, Y. Egashira, K. Ueyama, Catal. Letters 127 (2009) pp. 233–238.

[30] B. Vora, T.L. Marker, P.T. Barger, US Patent 6049017 (2000).

[31] N. Liu, S. Ding, Y. Cui, N. Xue, L. Peng, X. Guo, W. Ding, Chem. Eng. Res. Des. 91 (2013) pp. 573–580.

[32] M.M.J. Treacy, J.B. Higgins, Powder Patterns, in: Collection of Simulated XRD powder Patterns for Zeolites (Fourth Revised Eds.), Elsevier, Amsterdam, 2001, pp. 236–239.

[33] C. Baerlocher, L.B. McCusker, D.H. Olson, Framework Type Data Sheets, in: Atlas of Zeolite Framework Types(Sixth Revised Eds.), Elsevier, Amsterdam, 2007, p. 213

[34] T.A.J. Hardenberg, L. Mertens, P. Mesman, H.C. Muller, C.P. Nicolaides, Zeolites 12 (1992) pp. 685–689.

[35] F. Feng, K.J. Balkus, Microporous Mesoporous Mater. 69 (2004) pp. 85–96.

[36] R.A. Shaikh, S.G. Hegde, A.A. Behlekar, B.S. Rao, Catal. Today 49 (1999) pp. 201–209.

[37] W.F. Hölderich, J. Röseler, G. Heitmann, A.T. Liebens, Catal. Today 37 (1997) pp. 353–366.

[38] X. Tang, H. Zhou, W. Qian, D. Wang, Y. Jin, F. Wei, Catal. Letters 125 (2008) pp. 380–385.

[39] A. Corma, A. V. Orchillés, Microporous Mesoporous Mater. 35–36 (2000) pp. 21–30.

[40] A. Miyaji, Y. Sakamoto, Y. Iwase, T. Yashima, R. Koide, K. Motokura, T. Baba, J. Catal.

302 (2013) pp. 101–114.

VITAE

Name	Amr Abdalla Ibrahim Abdalla
Nationality	Sudanese.
Date of Birth	02/28/1991
Email	orma91@hotmail.com.com
Address	P. O. Box: 7422, King Fahd University of Petroleum & Minerals, Dhahran, Eastern Province, 31261 Saudi Arabia.
Academic Background	Bachelor of Science, Chemical Engineering (2007-2012) University of Khartoum, Sudan.
Publications	Conference Proceedings: Abdalla A., Palani A., Al-Khattaf S., Active and stable catalyst for 1-butene cracking to propylene, Proceedings 26th Saudi-Japan Annual Symposium, Dhahran Saudi Arabia, Nov. 7-8, 2016.